Whole-Exome Sequencing for Variant Discovery in Blepharospasm

Jun Tian,[1,2] Satya R. Vemula,[1,11] Jianfeng Xiao,[1,11] Enza Maria Valente,[3,4] Giovanni Defazio, [5,6] Simona Petrucci,[7] Angelo Fabio Gigante,[5] Monika Rudzińska-Bar,[8] Zbigniew K. Wszolek,[9] Kathleen D. Kennelly,[9] Ryan J. Uitti,[9] Jay A. van Gerpen,[9] Peter Hedera,[10] Elizabeth J. Trimble,[1] and Mark S. LeDoux[1,*]

[1]Departments of Neurology and Anatomy and Neurobiology, University of Tennessee Health Science Center, Memphis, TN, 38163, USA;

[2]Department of Neurology, Second Affiliated Hospital, School of Medicine, Zhejiang University, Hangzhou, Zhejiang, 310009, P.R. China;

[3]Department of Molecular Medicine, University of Pavia, 27100 Pavia PV, Italy

[4]Neurogenetics Unit, IRCCS Santa Lucia Foundation, 00143 Rome RM, Italy;

[5]Department of Basic Clinical Sciences, Neuroscience and Sense Organs, Aldo Moro University of Bari, 70121 Bari BA, Italy;

[6]Department of Medical Sciences and Public Health, University of Cagliari, Italy.

[7]Department of Neurology and Psychiatry, Sapienza University of Rome, 00185 Rome RM, Italy

[8]Department of Neurology, Faculty of Medicine, Medical University of Silesia, 40-752 Katowice, Poland;

[9]Department of Neurology, Mayo Clinic Florida, Jacksonville, FL, 32224, USA;

[10]Department of Neurology, Vanderbilt University, Nashville, TN, 37240, USA;

[11] These authors contributed equally to this work

24 *Correspondence: University of Tennessee Health Science Center, Department of
25 Neurology, 855 Monroe Avenue, Suite 415 Link Building, Memphis, TN, 38163, USA
26 Tel.: 901-448-1662, E-mail address: mledoux@uthsc.edu

27

28

Abstract

Background: Blepharospasm (BSP) is a type of focal dystonia characterized by involuntary orbicularis oculi spasms that are usually bilateral, synchronous, and symmetrical. Despite strong evidence for genetic contributions to BSP, progress in the field has been constrained by small cohorts, incomplete penetrance, and late age of onset. Although several genetic etiologies for dystonia have been identified through whole-exome sequencing (WES), none of these are characteristically associated with BSP as a singular or predominant manifestation.

Methods: We performed WES on 31 subjects from 21 independent pedigrees with BSP. The strongest candidate sequence variants derived from *in silico* analyses were confirmed with bidirectional Sanger sequencing and subjected co-segregation analysis.

Results: Co-segregating deleterious variants (GRCH37/hg19) in *CACNA1A* (NM_001127222.1: c.7261_7262delinsGT, p.Pro2421Val), *REEP4* (NM_025232.3: c.109C>T, p.Arg37Trp), *TOR2A* (NM_130459.3: c.568C>T, p.Arg190Cys), and *ATP2A3* (NM_005173.3: c.1966C>T, p.Arg656Cys) were identified in four independent multigenerational pedigrees. Deleterious variants in *HS1BP3* (NM_022460.3: c.94C>A, p.Gly32Cys) and *GNA14* (NM_004297.3: c.989_990del, p.Thr330ArgfsTer67) were identified in a father and son with segmental cranio-cervical dystonia first manifest as BSP. Deleterious variants in *DNAH17*, *TRPV4*, *CAPN11*, *VPS13C*, *UNC13B*, *SPTBN4*, *MYOD1*, and *MRPL15* were found in two or more independent pedigrees. To our knowledge, none of these genes have previously been associated with isolated BSP, although other *CACNA1A* mutations have been associated with both positive and

negative motor disorders including ataxia, episodic ataxia, hemiplegic migraine, and dystonia.

Conclusions: Our WES datasets provide a platform for future studies of BSP genetics which will demand careful consideration of incomplete penetrance, pleiotropy, population stratification, and oligogenic inheritance patterns.

KEYWORDS blepharospasm, cerebellum, dystonia, Purkinje cell, whole-exome sequencing

1 INTRODUCTION

Dystonia is defined as a movement disorder characterized by sustained or intermittent muscle contractions causing abnormal, often repetitive, movements, postures, or both (Albanese et al., 2013). In general, adult- or late-onset dystonia without evidence of overt degeneration or structural lesions of the nervous system is referred to as isolated dystonia and can be inherited in an autosomal-dominant fashion with reduced penetrance. The most common forms of focal dystonia are cervical dystonia and blepharospasm (BSP). Blepharospasm (BSP) (OMIM: 606798) is characterized by involuntary orbicularis oculi spasms that are usually bilateral, synchronous, and symmetrical (Defazio et al., 2015). Review of BSP epidemiological data provides prevalence estimates ranging from 16 to 133 per million (Defazio, Abbruzzese, Livrea, & Berardelli, 2004). BSP is significantly more common in females (>2F:1M) with a mean age of onset at approximately 55 years (O'Riordan et al., 2004). In comparison to cervical and laryngeal dystonia, BSP is more likely to spread to other body parts (Weiss et al., 2006). Most commonly, BSP spreads to contiguous craniocervical segments (lower face, masticatory muscles, and neck). The term segmental craniocervical dystonia is applied to the combination of BSP and dystonia of other head and neck muscles (LeDoux, 2009). Herein, BSP-plus (BSP+) will be used to denote subjects with BSP who exhibit subsequent spread to other anatomical segments (LeDoux, 2009; Waln & LeDoux, 2011). Sensory tricks or geste antagonistes are highly specific to dystonia, reported in a high percentage of patients with BSP, and can facilitate the diagnosis of BSP (Defazio, Hallett, Jinnah, & Berardelli, 2013). However, without valid

genetic biomarkers, the diagnosis of BSP can be difficult, even for experienced clinicians (Defazio et al., 2013).

Although rare cases of isolated BSP have been linked to *THAP1* (OMIM 609520) mutations (LeDoux et al., 2012; Vemula et al., 2014), the genetic underpinnings of this focal dystonia remain largely unknown. In one study, 233 relatives of 56 probands with primary BSP were examined and 27% had a first-degree relative affected by BSP or other dystonia (Defazio, Martino, Aniello, Masi, Abbruzzese, et al., 2006). Using an autosomal dominant model, penetrance was approximately 20% in pedigrees with BSP (Defazio, Martino, Aniello, Masi, Abbruzzese, et al., 2006; Defazio, Martino, Aniello, Masi, Gigante, et al., 2006). For comparison, penetrance of the classic ΔGAG mutation in *TOR1A* (OMIM 605204, DYT1) is 30-40% (Bressman et al., 2000). Approximately 10% of subjects in large biorepositories of isolated dystonia have a first- or second-degree relative with dystonia (LeDoux et al., 2016; Vemula et al., 2013; Vemula et al., 2014; Xiao et al., 2012; Xiao et al., 2011; Xiao et al., 2010). Even though late-onset isolated dystonia has a considerable “heritable” component, large pedigrees adequately powered for linkage analysis are rare. Conversely, small multiplex pedigrees with 2 or 3 affected individuals are not uncommon.

In six published clinical series, 1st-degree relatives of probands with isolated dystonia were subjected to examination (Defazio, Livrea, Guanti, Lepore, & Ferrari, 1993; Defazio, Martino, Aniello, Masi, Abbruzzese, et al., 2006; Leube, Kessler, Goecke, Auburger, & Benecke, 1997; Stojanovic, Cvetkovic, & Kostic, 1995; Waddy, Fletcher, Harding, & Marsden, 1991). Within these reported families, overall phenotypic concordance-discordance was approximately 50%-50%. However, discordant

104 pedigrees are relatively more common in probands with BSP than cervical dystonia
105 (Defazio, Berardelli, & Hallett, 2007). An example of phenotypic discordance would be
106 the presence of BSP in a proband and cervical dystonia in one of the proband's siblings.
107 Phenotype concordance is the presence of a single anatomical distribution of dystonia
108 (e.g., BSP) in all affected family members.

109 Herein, we report the results of whole-exome sequencing (WES) of 31 subjects
110 from 21 independent pedigrees with BSP and/or BSP+, the largest collection of BSP
111 pedigrees examined to date. Our series includes both concordant and discordant
112 pedigrees. Our results will facilitate a better understanding of the genetic underpinnings
113 of isolated BSP and other, mainly adult-onset, dystonias. A collection of *in silico* tools
114 including dbNSFP (Dong et al., 2015; Liu, Jian, & Boerwinkle, 2011; Liu, Wu, Li, &
115 Boerwinkle, 2016), dbscSNV (Jian, Boerwinkle, & Liu, 2014), Combined Annotation-
116 Dependent Depletion (CADD) (Kircher et al., 2014), REVEL (Ioannidis et al., 2016), and
117 MutationTaster (Schwarz, Cooper, Schuelke, & Seelow, 2014) were used to identify and
118 prioritize candidate sequence variants. Putative disease-associated variants were
119 confirmed with bidirectional Sanger sequencing, followed by co-segregation analysis.
120 Co-segregating deleterious variants in *CACNA1A* (OMIM 601011), *REEP4* (OMIM
121 609349), *TOR2A* (OMIM 608052), *ATP2A3* (OMIM 601929), *HS1BP3* (OMIM 609359),
122 *GNA14* (OMIM 604397) and *DNAH17* (OMIM 610063) were identified in single
123 pedigrees.
124
125
126 **2 MATERIALS AND METHODS**

127 **2.1 Ethical compliance**

128 All human studies were conducted in accordance with the Declaration of Helsinki with
129 formal approval from the University of Tennessee Health Science Center Institutional
130 Review Board (IRB) (01-07346-FB, 05-08331-XP, and 14-03320-XP) and ethics
131 committees of all participating centers. All subjects gave written informed consent for
132 genetic analyses and disclosure of medical information.

133

134 **2.2 Subjects**

135 Subjects in this study were examined by at least one neurologist with subspecialty
136 expertise in movement disorders. Subjects were asked to perform specific tasks
137 including holding their eyes open, opening and closing their eyes gently, opening and
138 closing their eyes forcefully, along with additional verbal and postural maneuvers
139 designed to capture masticatory, laryngeal or cervical involvement. A clinical diagnosis
140 of definite BSP was given to subjects that exhibited increased blinking and stereotyped,
141 bilateral and synchronous orbicularis oculi spasms inducing narrowing/closure of the
142 eyelids (Defazio et al., 2013). Subjects with isolated episodes of increased eyelid
143 blinking were given a diagnosis of possible BSP. Each affected or possibly affected
144 family member was queried for the presence of sensory tricks. WES was completed on
145 a total of 31 subjects from 21 pedigrees from the United States, Poland, and Italy (Table
146 1). Prior to WES, pathogenic variants in *THAP1*, *GNAL* (OMIM 139312) and Exon 5 of
147 *TOR1A* were excluded as previously described (LeDoux et al., 2012; Vemula et al.,
148 2013; Xiao et al., 2009; Xiao et al., 2010). Two pedigrees were African-American and
149 nineteen pedigrees were Caucasian of European descent. The results of WES on the

150 proband of African-American pedigree 10908 were previously reported (Xiao,
151 Thompson, Vemula, & LeDoux, 2016) and deposited in Sequence Read Archive
152 (SRX1790848).
153

154 **2.3 Whole-Exome Sequencing**

155 The concentration and quality of genomic DNA (gDNA) extracted from peripheral blood
156 were examined with a NanoDrop® ND-1000 (Thermo Scientific), the Qubit® dsDNA BR
157 Assay Kit (Thermo Scientific) and agarose gel electrophoresis. DNA was then
158 forwarded to Otogenetics or Beijing Genomics Institute (BGI) for additional in-house
159 quality control assessments prior to WES.

160 For WES at Otogenetics, 3 μg of genomic DNA (gDNA) was sheared to yield 100 -
161 450 bp fragments. In-solution whole-exome capture and massively parallel sequencing
162 was performed using the Agilent SureSelect^{XT} All Exon Kit 51 Mb. Enriched DNA
163 fragments were sequenced on Illumina's HiSeq 2500 platform as paired-end 100 to 125
164 base-pair reads. On average, over 95% of exons were covered at > 20X. The
165 percentage of exome coverage was based on exons targeted by the 51 Mb All Exon v4
166 Kit which incorporates Consensus Coding Sequence (CCDS), NCBI Reference
167 Sequence (RefSeq) and GENCODE annotations.

168 For WES at BGI, the gDNA samples were fragmented by Covaris, and, after two
169 rounds of bead purification, the resulting gDNA fragments were mainly distributed
170 between 200 to 400 bp. Then, AdA 5'- and 3'-adaptors were ligated to the 5'- and 3'-
171 ends of the fragments, respectively. The AdA adaptor-ligated fragments were amplified
172 by PCR, and the PCR products were used for exon capture. A 58.95 Mb region was

173 targeted for capture. The captured exon fragments were purified by DynabeadsM-280
174 streptavidin bead purification and were further amplified by another round of PCR.
175 Then, the PCR products were circularized and the resulting double strand (ds) circles
176 digested with *Ecop15*. Among these digested fragments, small fragments were
177 collected after bead purification. Similar to the AdA adaptor ligation, AdB adapters were
178 ligated to both ends of the purified fragments and the fragments were then used for
179 single strand (ss) circularization. The resulting ss circles were the final library products
180 used on the CG Black Bird sequencing platform. Finally, high-throughput sequencing
181 was performed for each captured library.
182

183 **2.4 Read Mapping**

184 Sequence reads (FASTQ) from Illumina (Otogenetics) were mapped to the human
185 reference genome (NCBI build 37.1) with NextGENe® (SoftGenetics). Using the
186 consolidation and elongation functions of NextGENe, instrument sequencing errors
187 were reduced and sequence reads were lengthened prior to variant analysis. The
188 condensation tool polished the data for adequate coverage by clustering similar reads
189 with a unique anchor sequence. Using this process, short reads were lengthened and
190 reads with errors were filtered or corrected. To maximize the probability of detecting
191 causal variants, all base changes occurring in ≥ 4 reads in any individual sample were
192 classified as variants for downstream analyses. An Overall Mutation score of 5 was
193 used as a cut-off to filter read errors and reduce the effects of allelic imbalances. The
194 Overall Mutation score is generated via a proprietary algorithm (SoftGenetics) to provide
195 an empirical estimation of the likelihood that a given variant call is genuine and not an

196 artifact of sequencing or alignment errors. This score is based on the concept of Phred
197 scores, where quality scores are logarithmically linked to error probabilities. With
198 NextGENe® software, intergenic and deep intronic [≥ 12 nt from splice sites] variants
199 were eliminated prior to downstream in silico analyses.

200 Complete Genomics (BGI) developed high-speed mapping software capable of
201 aligning read data to reference sequences. Using GRCh37 as the reference, the
202 mapping is tolerant of small variations from a reference sequence, such as those
203 caused by individual genomic variation, read errors, or unread bases. To support
204 assembly of larger variations, including large-scale structural changes or regions of
205 dense variation, each arm of a DNA Nanoball (DNB) is mapped separately, with mate
206 pairing constraints applied after alignment. Initially, mapping reads to the human
207 reference genome is a constrained process that does not allow for insertions and
208 deletions. All mate-pair constraint-satisfying paired-end mappings are used to detect
209 small variants. DNBs are then filtered and individual reads are optimized. Optimization
210 collects reads likely to lie in regions of interest using mate alignment information and
211 performs local *de novo* assemblies.

212

213 **2.5 Single-Nucleotide Variants (SNVs) and Small Insertions and Deletions**
214 **(INDELS)**

215 First, a list of shared variants was generated for pedigrees with two or more affected
216 subjects analyzed with WES. For Otogenetics Illumina data, we eliminated SNVs and
217 INDELS with minor allele frequencies (MAFs) ≥ 0.001 in the Exome Aggregation
218 Consortium (ExAC) (Lek et al., 2016) database or 1000 Genomes (1KG), variants with

219 unbalanced reads (variant allele < 25%), and regions covered by < 5 reads. For BGI
220 data, we eliminated SNVs and INDELs with MAFs ≥ 0.001 in 1 KG or Exome Variant
221 Server (EVS). Of note, both BGI and Otogenetics outputs contain inverted major/minor
222 allele classifications for a subset of sequence variants (minor allele: MAF < 0.001 or >
223 0.999). All nonsynonymous SNVs were analyzed with dbNSFP (versions 3.3 to 3.5)
224 (Liu et al., 2016), CADD (Kircher et al., 2014) and REVEL (Ioannidis et al., 2016).
225 Nonsynonymous SNVs with MetaLR (Dong et al., 2015) ranking scores > 0.75, CADD
226 phred scores > 15, or REVEL scores > 0.5 were retained for further evaluation.
227 Nonsense SNVs, frameshift variants, synonymous SNVs, splice site SNVs, and other
228 SNVs and INDELS (3' and 5' untranslated region [UTR] variants, downstream variants,
229 intronic variants, noncoding variants and upstream variants) were analyzed with CADD
230 +/- MutationTaster2 (Schwarz, Rodelsperger, Schuelke, & Seelow, 2010). Nonsense
231 SNVs, frameshift variants, synonymous SNVs, splice site SNVs, other SNVs and
232 INDELs with CADD_phred scores > 15 were retained for further evaluation. All splice-
233 site SNVs were analyzed with dbscSNV1.1 (Jian et al., 2014), which contains pre-
234 computed ensemble scores, Ada and RF, for all potential splice-site SNVs computed
235 using AdaBoost and random forests, respectively. Splice-site SNVs with Ada scores >
236 0.6 or RF scores > 0.6 were retained for further evaluation. Particular attention was
237 paid to variants within the DYT13 (1p36.32-p36.13) (Bentivoglio et al., 1997; Valente et
238 al., 2001) and DYT21 (2q14.3-q21.3) loci. The DYT13 locus was identified via linkage
239 analysis of a large 3-generation pedigree with craniocervical and other anatomical
240 distributions of dystonia. Similarly, the DYT21 locus was defined through linkage
241 analysis of a Swedish kindred with apparently autosomal dominant inheritance of

242 dystonia which included BSP is several affected subjects (Forsgren, Holmgren, Almay,
243 & Drugge, 1988; Norgren, Mattson, Forsgren, & Holmberg, 2011). Detailed methods for
244 analysis of BGI and Otogenetics information can be found in the Supplemental Data.
245 REVEL, MetaLR and CADD scores were used to prioritize nonsynonymous
246 missense variants for additional scrutiny whereas CADD and ExAC Probability of Loss-
247 of-Function (LoF) intolerance (pLI) scores were used to prioritize nonsense SNVs and
248 frameshift INDELs. MutationTaster was also used for analysis of small INDELs which
249 are not scored by REVEL or MetaLR. Each category of variant (nonsynonymous,
250 synonymous, splice-site, nonsense, frameshift, other INDELs, and other SNVs) was
251 ranked by *in silico* scores of deleteriousness. Population frequencies for the highest
252 scoring variants were additionally assessed with genome Aggregation Database
253 (gnomAD), NHLBI Exome Sequencing Project (ESP) Exome Variant Server (EVS) with
254 particular attention to racial subcategories. All NCBI databases were queried with gene
255 symbols and the names of encoded proteins. Particular attention was paid to data
256 contained in PubMed, ClinVar, OMIM, and BioSystems. OMIM was searched for allelic
257 disorders/phenotypes. MARRVEL and its link outs were used to explore available data
258 related to animal models of homologues, genomic structural variants (DGV and
259 DECIPHER), gene expression (GTex), and protein expression (ProteinAtlas). Gene
260 expression was also analyzed with Allen Brain Atlas and BioGPS. Candidate genes
261 were eliminated if not expressed in at least one “motor” region of the brain (striatum,
262 cerebellum or frontal motor cortex). UniProt was used to access protein-protein
263 interactions, sites of known or predicted post-translational modifications and known or
264 putative protein functions. Multiple sequence alignments were performed with Clustal

265 Omega. A subset of candidate pathogenic variants was confirmed with bidirectional
266 Sanger sequencing to exclude next generation sequencing read errors. After Sanger
267 confirmation, co-segregation was assessed in individual pedigrees.
268

269 **2.6 Copy Number Variant Analysis**

270 CNVkit (Talevich, Shain, Botton, & Bastian, 2016), a Python library and command-line
271 software toolkit to infer and visualize copy number variants (CNVs) from targeted DNA
272 sequencing data, was used to detect CNVs in WES data generated by Otogenetics on
273 the Illumina platform. CNVkit was designed for use on hybrid capture sequencing data
274 where off-target reads are present and can be used to improve copy number estimates.
275 CNVkit normalizes read counts to a pooled reference and corrects for three main
276 sources of bias: GC content, target footprint size, and repetitive sequences. For this
277 purpose, Otogenetics provided us with WES data from 15 random subjects of unknown
278 race and unknown geographic region of origin sequenced as part of unrelated projects
279 using the Agilent SureSelect^{XT} All Exon Kit 51 Mb for exome capture and sequenced on
280 Illumina's HiSeq 2500 platform.

281 CNVkit reports log2 copy ratios. Assuming pure samples and germline mutations,
282 the log2 ratio should be -1.0 for a deletion mutation and infinity if both alleles are
283 deleted. The log2 ratio is 0.585 for duplications and 1.0 for triplications. The
284 relationship between the estimated copy number and the true copy number depends on
285 a number of factors including read depth and number of probes covering a region of
286 interest.
287

288 **2.7 Sanger Sequencing**

289 PCR was performed using 40 ng of peripheral blood gDNA along with 200 nM of each
290 primer (Table S1) in a 10-µl reaction volume with HotStarTaq® Plus DNA polymerase
291 from Qiagen. The following cycling conditions were employed: 95°C for 15 min; 35
292 cycles at 95°C for 10 s, 58°C for 30 s, and 72°C for 30 s.

293

294 **2.8 PCR Validation of Copy Number Variants**

295 Quantitative PCR (qPCR) was used for initial assessment of a random selection of
296 predicted CNVs identified with CNVkit. Primers and probes for qPCR were designed
297 with Roche's Universal Probe Library to cover (Table S1). qPCR was performed using
298 20 ng of template DNA and 200 nM of each primer in a 10-µl reaction volume with the
299 LightCycler™ 480 system and Universal Taqman® probes (Roche). The following cycling
300 conditions were employed: 95°C for 5 min; 45 cycles at 95°C for 10s, 58°C for 30s, and
301 72°C for 12s. Copy numbers were calculated against an endogenous control, *HLCS*,
302 holocarboxylase synthetase. All assays were carried out in triplicate and means were
303 used for calculating fold changes.

304 Digital PCR (dPCR) was then used for confirmation of select deletion and
305 duplication CNVs identified with CNVkit. Literature mining as described for SNVs and
306 small INDELs was used to select genes with deletion log2 scores of -0.75 to -1.25 and
307 covered by ≥ 4 probes, or genes with duplication log2 scores of 0.385 to 0.835 and
308 covered by ≥ 4 probes. Primers and probes (FAM dye-labeled) were designed via
309 Roche's Universal Probe Library to encompass the estimated deletion regions (Table
310 S1). The TaqMan copy number reference assay (Applied Biosystems 4403326)

311 contained RNase P-specific forward and reverse primers and VIC dye-labelled TAMRA
312 hydrolysis probe. RNase P, a single copy gene, is used as the reference for this work
313 (Qin, Jones, & Ramakrishnan, 2008).
314 Reaction mixtures (4.0 µl) containing TaqMan gene-expression master mix (Life
315 Technologies), 20X GE sample loading reagent (Fluidigm 85000746), 20X gene-specific
316 assays, 20X TaqMan copy number reference assay (Applied Biosystems) and 1.2 µl
317 target gDNA (20 ng/µl) was pipetted into each loading inlet of a 48.770 dPCR array
318 (Fluidigm). The BioMark IFC controller MX (Fluidigm) was used to uniformly partition the
319 reaction from the loading inlet into the 770X0.84 nl chambers and dPCR was performed
320 with the Fluidigm BioMark System for Genetic Analysis. The Fluidigm dPCR software
321 was used to count gene copy numbers. The quality thresholds were manually set
322 specific to each assay, but consistent across all panels of the same assay. The CNV
323 calculation is based on "relative copy number" so that apparent differences in gene copy
324 numbers in different samples are not distorted by differences in sample amounts. The
325 relative copy number of a gene (per genome) is expressed as the ratio of the copy
326 number of a target gene to the copy number of a single copy reference gene in the
327 sample. By using assays for the two genes (the gene of interest and the reference
328 gene) with two fluorescent dyes on the same Digital Array IFC, we are able to
329 simultaneously quantitate both genes in the same DNA sample. The ratio of these two
330 genes is the relative copy number of the gene of interest.

331

332 **2.9 Data Availability**

333 Primers (Table S1), WES variants examined with Sanger sequencing (Table S2), and
334 potential CNVs examined with qPCR (Table S3) are included in Supplemental Data.
335 Comprehensive WES variant analysis for each pedigree is included in individual Excel
336 workbooks (10012, 10014, 10035, 10036, 10043, 10064, 10076, 10178, 10193, 10274,
337 10455, 10908, 25056, 25069, 25215, 45263, 85020, NB0362_BGI, NG0369, NG0450,
338 and NG1072_BGI).
339
340
341 **3 RESULTS**
342
343 **3.1 BSP and BSP+ Pedigrees**
344
345 WES was completed on 31 subjects from 21 distinct pedigrees with either concordant or
346 discordant BSP and BSP+ phenotypes (Table 1, Figures 1 and 2, Supplemental Data).
347 Exome coverage is provided in Tables 2 and 3. Dept of coverage was ≥ 10x and ≥ 20x
348 for over 97.5% and 95% of the 31 exomes. Numbers of total and filtered variants are
349 provided in Table 4.
350
351 **3.2 *CACNA1A* INDEL in a Three-Generation Pedigree with BSP**
352 A novel *CACNA1A* INDEL (c.7261_7262delinsGT [NM_001127222.1], p.Pro2421Val
353 [NP_001120694.1]) was identified in three males and one asymptomatic female family
354 member from a three-generation pedigree with BSP (Figure 3, Tables 1, 5, 8 and S2;
355 Supplemental Data). Complete Genomics outputted this variant as two contiguous

356 SNVs. This INDEL is not reported in control databases (ExAC, 1KG or gnomAD) and
357 predicted to be deleterious by CADD (Phred score = 19.51) and MutationTaster
358 (disease causing, probability value: 1.0). However, two contiguous SNVs are reported
359 in gnomAD (19:13318386 and 19:13318387) with very similar allele frequencies
360 (211/118674 and 207/119456). Analysis of read data suggests that the majority of
361 these SNVs are, in fact, part of the c.7261-7262delinsGT INDEL. The
362 19:13318386G/A variant is present at relatively high frequency in the Finnish population
363 (1.49E-02) with a much lower allele frequency of (6.76E-04) in non-Finnish Europeans
364 and quite rare in other racial populations. The identified amino acid substitution is
365 located in the C-terminal, intracellular domain of the encoded voltage-dependent P/Q-
366 type calcium channel subunit α-1A, which is conserved among mammals (Figure 3).
367 We did not screen other variants for co-segregation given previously established
368 associations between *CACNA1A* and dystonia. Five SNVs had CADD_phred scores >
369 15 and REVEL scores > 0.5 but none had a MetaLR score > 0.75, REVEL score > 0.75
370 and CADD_phred score > 30. A frameshift INDEL in *MMP28* with a CADD_phred score
371 of 34 is reported in ExAC and gnomAD. Four nonsense SNVs had CADD_phred scores
372 > 30 but two are reported in ExAC and gnomAD and none seem biologically plausible
373 candidates.
374

375 **3.3 *REEP4* Missense Variant**

376 A nonsynonymouse SNV in *REEP4* (c.109C>T [NM_025232.3], p.Arg37Trp
377 [NP_079508.2]) was identified in seven subjects with BSP+ or BSP and one
378 asymptomatic female family member from a three-generation African-American

379 pedigree (Figure 4, Tables 1, 5, 8 and S2; Supplemental Data). This variant is present
380 at very low frequency in gnomAD and predicted to be deleterious by *in silico* analysis
381 including CADD (phred score = 34), REVEL (0.767), MetaLR (0.960), and
382 MutationTaster2 (disease causing, probability value: 1.0). In gnomAD, this variant is not
383 present in 15,290 African alleles. The p. Arg37Trp variant alters an amino acid that is
384 highly conserved among vertebrates as shown by the multiple pairwise alignments
385 generated with Clustal Omega (Figure 4).
386

387 **3.4 *TOR2A* Missense Variant**

388 A *TOR2A* nonsynonymous SNV (c.568C>T [NM_130459.3], p.Arg190Cys
389 [NP_569726.2]) was identified in three subjects with BSP and three asymptomatic
390 members from a four generation pedigree (Figure 5; Tables 1, 5, 8 and S2;
391 Supplemental Data). This variant is present at low frequency in ExAC (5.84e-05) and
392 predicted to be deleterious by *in silico* analysis including CADD (phred score = 34),
393 REVEL (0.548), MetaLR (0.811), and MutationTaster2 (disease causing, probability
394 value: 1.0). The p.Arg190Cys variant alters an amino acid that is highly conserved
395 among vertebrates as shown by the multiple pairwise alignments generated with Clustal
396 Omega (Figure 5). *TOR2A* encodes torsin family 2 member, a known interactor with
397 dystonia-associated protein torsinA (BioGRID). Nonsense variants in *PCDH15* and
398 *GTDC1* were also detected in all three affected subjects and have CADD_phred scores
399 > 30 but pLI scores of 0. *PCDH15* and *GTDC1* have 28 and 15 LoF variants in ExAC,
400 respectively. *FRG1* variants detected with WES are likely due to mapping errors
401 caused by related genomic sequences.

402

403 **3.5 *ATP2A3* Missense Variant**

404 An *ATP2A3* nonsynonymous SNV (c.1966C>T [NM_005173.3], p.Arg656Cys
405 [NP_001120694.1]) was identified in five affected subjects, one possibly affected
406 subject, and three asymptomatic members of discordant Family NG1072 (Figure 5;
407 Tables 1, 5, 8 and S2; Supplemental Data). Predicted to be highly deleterious by all *in*
408 *silico* analysis (CADD_phred score = 34, REVEL score = 0.872, MetaLR = 0.99175,
409 MutationTaster2 [disease causing, probability value: 1.0]), this variant (rs140404080) is
410 reported in ExAC (5.51E-04) and gnomAD (6.63E-04) with a population frequency of
411 approximately 0.1%. The Arg656Cys variant alters an amino acid that is highly
412 conserved among vertebrates (Figure 5). Another candidate variant in *MYH13*
413 (rs7807826) did not completely co-segregate with dystonia in this pedigree (Table S2,
414 Supplemental Data). Moreover, expression of *MYH13* is mainly restricted to the
415 extrinsic eye muscles. A nonsense variant in *NOS2* (NM_000625.4: c.2059C>T,
416 p.Arg687*; CADD_phred = 36) was shared by the two affected individuals analyzed with
417 WES but *NOS2* is expressed at only low levels in brain and *Nos2*$^{-/-}$ mice have not been
418 reported to manifest positive or negative motor signs. *ATP2A3* is highly expressed in
419 cerebellar Purkinje cells (Allen Brain Atlas) and is a member of the P-type ATPase
420 superfamily that includes the gene (*ATP1A3*) causally-associated with rapid-onset
421 dystonia-Parkinsonism (DYT12).

422

423 **3.6 *GNA14* and *HS1BP3* Variants in Pedigree with BSP+ and Parkinsonism**

424 A novel *HS1BP3* nonsynonymous SNV (c.94C>A [NM_022460.3], p.Gly32Cys
425 [NP_071905.3]) was found in a father and son with severe BSP+ (Family 10043) (Figure
426 6; Tables 1, 5, 8 and S2; Supplemental Data). The deceased father had two brothers
427 with clinical diagnoses of Parkinson disease (PD). The proband has BSP, mild lower
428 facial dystonia, cervical dystonia and laryngeal respiratory dystonia. The laryngeal
429 respiratory dystonia required treatment with a tracheostomy. The proband developed
430 levodopa-responsive Parkinsonism approximately 15 years after the onset of his
431 dystonia. An ioflupane I-123 dopamine transporter scan showed nigrostriatal
432 denervation. The c.94C>A [NM_022460.3] variant is not reported in ExAC, 1KG or
433 gnomAD, and is predicted to be deleterious by all *in silico* analysis (CADD_phred score
434 = 34, REVEL = 0.454, MetaLR = 0.803). Of note, a different variant in *HS1BP3*
435 (p.A265G) was previously associated with essential tremor (ET), a disorder potentially
436 related to the adult-onset dystonias through common genetics (Higgins et al., 2005).
437 The p.Gly32Cys variant alters an amino acid that is highly conserved among
438 vertebrates (Figure 6).
439 A *GNA14* frameshift variant (c.989_990del [NM_004297.3], p.Thr330ArgfsTer67
440 [NP_004288.1]) was also identified in the same pedigree (Family 10043) and is present
441 at low frequency in gnomAD (1.23E-05) (Figure 6; Tables 1, 5, and 8 and S2;
442 Supplemental Data). This *GNA14* variant is predicted to be deleterious by CADD
443 (phred score = 36) and MutationTaster2 (disease causing, probability value: 1.0).
444 *GNA14* encodes G protein subunit α14 which shows modest expression in brain,
445 particularly the striatum and cerebellum (Human Protein Atlas). Recently, somatic
446 mutations in *GNA14* have been linked to congenital and sporadic vascular tumors (Lim

et al., 2016). Mutations in another G protein, Gα(olf), are associated with various anatomical distributions of mainly adult-onset dystonia.

3.7 *DNAH17* Variants Found in Pedigree and Isolated Subject with BSP

Deleterious variants in *DNAH17* were identified in two brothers with BSP and one isolated case of BSP (Figure 7; Table 1, 6, 8 and S2, Supplemental Data). Both variants are present at low frequency in ExAC and gnomAD. *DNAH17* encodes dynein axonemal heavy chain 17. The FANTOM5 dataset reports expression of *DNAH17* in testes and brain (hippocampus, caudate and cerebellum) (Kawaji, Kasukawa, Forrest, Carninci, & Hayashizaki, 2017). *DNAH17* has not yet been linked to any other neurological or non-neurological disease. A roundworm homolog (*dhc-1*) of human *DNAH17* is involved in cytokinesis, microtubule-based movement, mitotic spindle organization, meiotic nuclear division and nervous system development (MARRVEL).

3.8 Copy Number Variants

CNVkit called from 11 to 217 CNVs per shared exome. Assessing randomly selected CNVs with qPCR showed high discordancy (Table S3), particularly for variants that did not have log2 ratios near -1.0. We then focused on CNVs with log2 ratios compatible with a single-copy gain (~0.585) or single-copy loss (-1.0) using dPCR. Deletions in *LILRA3* were confirmed in three unrelated subjects with BSP (Table 7). *LILRA3* (OMIM 604818) deletions are common in the general population and may increase risk for HIV infection and some autoimmune disorders (Ahrenstorf et al., 2017; Du et al., 2015). A deletion in *BTNL3* (OMIM 606192) and duplications in *SLC2A14* (OMIM 611039) ,

470 *SLC2A3* (OMIM 138170), *TOP3B* (OMIM 603582), and *UNK* (616375) were identified in
471 single exomes (Tables 7 and 8). *UNK* is expressed at high levels in brain (Allen Brain
472 Atlas, BioGPS, and The Human Protein Atlas) and plays an important role in the
473 development of neuronal morphology. Two *UNK* duplications are reported in ExAC. To
474 date, UNK has not been linked to any medical disorder (OMIM). Copy number analysis
475 of *GOLGA8A* (Chr15) was compromised by the presence of pseudogenes and a
476 homolog with very close sequence similarity on Chr15.
477

478 **3.9 Other Candidate Genes Found in Two or More Pedigrees**

479 The strongest candidate variants (CADD_phred > 20 and MutationTaster2 = disease
480 causing +/- MetaLR > 0.5) were compared among all exomes from all pedigrees to
481 identify common candidate genes. Three variants in *TRPV4* (OMIM 605427) were
482 identified in three independent pedigrees. *TRPV4* has been associated with several
483 medical disorders including autosomal dominant spinal muscular atrophy. However, all
484 three variants are reported in ExAC and gnomAD at significant frequencies. The same
485 SNV in *CAPN11* (OMIM 604822; NM_007058.3: c.425T>C, p.Leu142Pro) found in two
486 independent pedigrees is reported once in gnomAD and has high CADD_phred (32),
487 MetaLR (0.982) and REVEL (0.918) scores. *CAPN11* encodes calpain 11, an
488 intracellular calcium-dependent cysteine protease that shows highest expression in
489 testis. One nonsense variant in *VPS13C* (OMIM 608879) was found in a single subject
490 with BSP and a rare missense variant in *VPS13C* was found in another subject with
491 BSP. Both of these *VPS13C* variants are predicted to be highly deleterious to protein
492 function. Loss of VPS13C causes mitochondrial dysfunction and has been linked to

493 autosomal recessive PD (Lesage et al., 2016). Moreover, *VPS13C* variants may
494 increase risk for PD, in general (Foo et al., 2017), and, dystonia may share genetic
495 underpinnings with PD (LeDoux et al., 2016). Other candidate genes (*SPTBN4* [OMIM
496 606214], *MRPL15* [OMIM 611828], *UNC13B* [605836], and *MYOD1* [159970]) shared
497 by two pedigrees show moderate-to-high expression in motor regions of brain. Mice
498 carrying recessive loss-of-function *Sptbn4* mutations manifest ataxia, motor neuropathy,
499 deafness and tremor (Parkinson et al., 2001).
500

501 **3.10 DYT13 and DYT21 Loci**

502 Within the DYT13 locus (Chr1), three subjects harbored *ATP13A2* (OMIM 610513)
503 variants. Subject 10012 was found to have a missense variant (rs151117874,
504 CADD_phred = 22.4, REVEL = 0.497, MetaLR = 0.8657, gnomAD = 21/272174 [3.67E-
505 06], Supplemental Data). Less deleterious synonymous (CADD_phred = 17.53) and
506 missense (CADD_phred = 21.1) variants were found in subjects 10076 and 25069,
507 respectively (Table 1, Supplemental Data). Recessive mutations in *ATP13A2* have
508 been linked to Kufor-Rakeb syndrome (Ramirez et al., 2006) and spastic paraplegia 78
509 (Estrada-Cuzcano et al., 2017), both of which may include dystonia as a clinical
510 manifestation. Variants in *ATP13A2* may also contribute to oligogenic inheritance in PD
511 (Lubbe et al., 2016). In subject 10035, a deleterious variant within the DYT21 (Chr2)
512 locus was identified in *IMP4* (OMIM 612981; rs146322628, CADD_phred = 29.3,
513 MetaLR = 0.83, REVEL = 0.606, gnomAD = 5.1E-04, Supplemental Data), and
514 deleterious variants in *UBR4* (OMIM 609890; rs748114415, CADD_phred = 23.3,
515 REVEL = 0.188, MetaLR = 0.46, MutationTaster2 = 0.81 [disease causing], gnomAD =

516 5.1E-04, Supplemental Data), and *ARHGEF19* (OMIM 612496; rs144638812,
517 CADD_phred = 22.7, MetaLR = 0.64, REVEL = 0.11, MutationTaster2 = 0.55 [disease
518 causing], gnomAD = 2.3E-04, Supplemental Data) were identified in the DYT13 (Chr1)
519 locus. To date, *IMP4* and *ARHGEF19* have not been linked to a medical disorder.
520 IMP4 interacts with the U3 snoRNA complex and is involved in nucleolar function
521 (Granneman et al., 2003). A missense variant in *UBR4* (p.Arg5091His) was found to
522 segregate with episodic ataxia in a large Irish pedigree (Conroy et al., 2014). UBR4 is
523 expressed at high levels in cerebellar Purkinje cells (Allen Brain Atlas), interacts with
524 calmodulin, co-localizes with ITPR1, and may be involved in Purkinje cell calcium
525 homeostasis (Conroy et al., 2014). *ARHGEF19* shows significant expression in
526 cerebellar Purkinje cells (Allen Brain Atlas) and zebrafish *arhgef19* is involved in neural
527 tube closure (Miles et al., 2017).
528
529
530 **4 DISCUSSION**
531 The molecular and cellular mechanisms underlying BSP and other anatomical
532 distributions of isolated dystonia remain fragmentary. Accordingly, treatments for BSP
533 are entirely symptomatic (Pirio Richardson et al., 2017). Most commonly, BSP patients
534 are treated with injections of botulinum toxin although, in some series, almost 50%
535 report minimal improvement, no improvement or worsening of BSP after injections of
536 botulinum toxins (Fernandez et al., 2014). Identification of genetic etiologies for BSP
537 may permit development of targeted disease-modifying therapeutics. In this study, we

538 used exome sequencing to explore genetic contributions to BSP and provide a
539 foundation for future case-control studies of this important focal dystonia.
540 Although we do provide data suggesting potential roles for *CACNA1A, REEP4,*
541 *TOR2A, ATP2A3 HS1BP3/GNA14*, *DNAH17*, *TRPV4*, *CAPN11*, *VPS13C*, *UNC13B*,
542 *SPTBN4*, *MYOD1*, and *MRPL15* in the pathogenesis of BSP, the limitations of our work
543 should be bordered. First, we did not identify a common co-segregating genetic
544 etiology in more than one pedigree. This points to the likely genetic heterogeneity of
545 BSP but also suggests that one or more variants identified herein co-segregated by
546 chance alone. Unfortunately, none of our pedigrees were powered to generate LOD
547 (logarithm [base 10] of odds) scores > 3 thereby precluding the usage of linkage
548 analysis for validation of co-segregating variants. Second, several of the candidate
549 variants identified with WES are reported in population databases (ExAC and gnomAD)
550 with MAFs near the minimal population prevalence of BSP. On the other hand, noted
551 MAFs are significantly lower than the maximal population prevalence of BSP with
552 corrections for the markedly reduced penetrance characteristic of isolated dystonia.
553 Furthermore, BSP and premonitory increased blinking may be much more common in
554 the general population than commonly accepted (Conte et al., 2017). Thirdly, our
555 genetically-heterogeneous cohort included Polish, Italian, Caucasian-American and
556 African-American pedigrees, possibly reducing the probability of detecting variants
557 shared among pedigrees and singletons. Accordingly, follow-up case-control analysis
558 of individual variants identified herein will require careful attention to population
559 stratification and large sample sizes to confidently determine if variants in candidate
560 genes are enriched in BSP. Fourth, our prioritization of variants was predominantly

561 driven by *in silico* predictions of deleteriousness and many potentially-pathogenic
562 candidate variants were not confirmed with Sanger sequencing or subjected to co-
563 segregation analysis. Fifth, WES will miss most repeat expansions and does not
564 access the mitochondrial genome. In this regard, repeat expansions are a common
565 cause of late-onset neurological disease and mitochondrial mutations may include
566 dystonia as part of a more expansive neurological phenotype (LeDoux, 2012).
567 Furthermore, our approach to CNV analysis was largely insensate to smaller structural
568 variants such as single exonic deletions. Despite these limitations, our findings are
569 compatible with common themes in dystonia research (calcium signaling, Purkinje cells,
570 and dopaminergic signaling), point out potential genetic common ground with PD and
571 ET, suggest a role for oligogenic inheritance in BSP, and provide motivation for treating
572 a subset of BSP patients with acetazolamide.

573 *CACNA1A* is highly expressed in the cerebellum, particularly the Purkinje cell layer.
574 Mutations in several genes related to calcium signaling and homeostasis and expressed
575 in Purkinje cells have been causally associated with dystonia in humans and mice
576 (LeDoux, 2011). In fact, virtually all genes associated with dystonia in spontaneous
577 mutants (*tottering*, *stargazer*, *ophisthotonus*, *ducky*, *lethargic*, *waddles* and *wriggle*) are
578 involved in Purkinje cell Ca^{2+} signaling (*Canca1a, Cacng2, Itpr1, Cacna2d2, Cacnb4*
579 and *Pmca2*). In humans, autosomal-recessive mutations in *HPCA* (OMIM 142622)
580 cause childhood-onset dystonia and the encoded protein, hippocalcin, is robustly
581 expressed in Purkinje cells and serves as a Ca^{2+} sensor (Charlesworth et al., 2015;
582 Tzingounis, Kobayashi, Takamatsu, & Nicoll, 2007). SVs in *CACNA1A* have been
583 associated with a variety of neurological disorders including episodic ataxia type 2,

584 familial hemiplegic migraine, spinocerebellar ataxia type 6 (SCA6), and various
585 anatomical distributions of dystonia such as benign paroxysmal torticollis and infancy
586 and BSP (Naik, Pohl, Malik, Siddiqui, & Josifova, 2011; Sethi & Jankovic, 2002; Shin,
587 Douglass, Milunsky, & Rosman, 2016; S. D. Spacey, Materek, Szczygielski, & Bird,
588 2005; Thomsen et al., 2008). A notable percentage of patients with dystonia due to
589 mutations in *CACNA1A* show significant improvement with acetazolamide (S. Spacey,
590 1993; S. D. Spacey et al., 2005). Unfortunately, our pedigree was lost to follow-up and
591 none of the affected family members were treated with acetazolamide. The α-1 subunit
592 of P/Q type, voltage-dependent, calcium channel harbors a polyglutamine expansion in
593 its C-terminal intracellular domain and the novel missense variant p.Pro2421Val
594 identified in our pedigree with BSP is near this expansion (Figure 3). In contrast, the
595 previously described BSP-variant was likely associated with nonsense-mediated decay
596 and haploinsufficiency (S. D. Spacey et al., 2005). Mutations linked to familial
597 hemiplegic migraine appear to operate via gain-of-function mechanisms whereas the
598 SCA6 polyglutamine repeat and loss-of-function mutations may lead to neuronal cell
599 death (Cain & Snutch, 2011). In this context, it is worthy to note that reduced Purkinje
600 cell density was found in two individuals with BSP and cervical dystonia (Prudente et al.,
601 2013).

602 REEP4 is a microtubule-binding endoplasmic reticulum and nuclear envelope
603 protein (Schlaitz, Thompson, Wong, Yates, & Heald, 2013). Depletion of REEP4 from
604 HeLa cells is associated with defective cell division and proliferation of intranuclear
605 membranes derived from the nuclear envelope (Schlaitz et al., 2013). Similarly, omega-
606 shaped nuclear blebs have been used as a phenotypic measure of torsinA (encoded by

607 *TOR1A*) dysfunction (Laudermilch et al., 2016). In *Xenopus*, loss of REEP4 causes
608 defects of nervous system development and paralysis of embryos (Argasinska et al.,
609 2009). Mutations in *REEP1* (OMIM 609139) and *REEP2* (OMIM 609347) are
610 associated with spastic paraplegia (SPG) types 31 (SPG31), and 72 (SPG72).
611 Although dystonia is not a clinical feature typically reported in SPG31 and SPG72
612 cases, dystonia is not uncommon in several other SPGs including SPG7, SPG15,
613 SPG26, SPG35, and SPG47 (Klebe, Stevanin, & Depienne, 2015; van Gassen et al.,
614 2012).

615 A ΔGAG deletion in Exon 5 of *TOR1A* was the first SV to be linked to isolated
616 dystonia (Ozelius et al., 1997). TorsinA interacts with LAP1, a transmembrane protein
617 ubiquitously expressed in the inner nuclear membrane. Recessive mutations of
618 *TOR1AIP1* (OMIM 614512) which encodes LAP1 are associated with severe early-
619 onset generalized dystonia and progressive cerebellar atrophy (Dorboz et al., 2014).
620 Another torsinA interacting protein, torsin family 2 member A (encoded by *TOR2A*) was
621 found to harbor a missense variant in one of our pedigrees with BSP. Similar to the
622 ΔGAG mutation in *TOR1A*, the penetrance of the p.Arg190Cys missense variant
623 identified in our pedigree was less than 50%. *TOR2A* is a member of the human torsin
624 gene family (Laudermilch et al., 2016; Ozelius et al., 1999). *TOR1A*, *TOR2A* and
625 *TOR1AIP1* all show relatively high expression in cerebellar Purkinje cells (Allen Brain
626 Atlas).

627 A nonsynonymous SNV in *ATP2A3* (NM_005173.3: c.1966C>T, p.Arg656Cys) was
628 found in five definitely-affected subjects from a discordant pedigree with BSP from Italy.
629 However, this variant was not detected in one possibly affected family member with

630 writer's cramp. This could be either a phenocopy or evidence against the causality of
631 *ATP2A3*. Furthermore, the p.Arg656Cys variant is present at notably high frequency in
632 gnomAD (183/276114 alleles, no homozygotes, 0.13% of 138,057 subjects). BSP is the
633 most common focal dystonia in Italy with a crude prevalence rate of 133 per million or
634 0.013%. Even with a penetrance of < 20%, this suggests that p.Arg656Cys may not be
635 pathogenic or, at least, pathogenic in isolation, requiring digenic inheritance of another
636 pathogenic variant. On the other hand, p.Arg656Cys is predicted to be highly
637 deleterious, may contribute to other anatomical distributions of dystonia, and, like
638 *ATP1A3*, could be involved in the etiopathogenesis of other neurological disorders such
639 as Parkinson disease, Alzheimer disease, and brain tumors (Kawalia et al., 2017;
640 Korosec, Glavac, Volavsek, & Ravnik-Glavac, 2009; Matak et al., 2016). In this regard,
641 *ATP2A3* shows striking expression in cerebellar Purkinje cells and dopaminergic
642 neurons of the substantia nigra pars compacta (Allen Brain Atlas). *ATP2A3* encodes a
643 sarcoplasmic/endoplasmic reticulum Ca^{2+} ATPase and disorders of Purkinje cell
644 (LeDoux, 2011) and dopaminergic (Surmeier, Halliday, & Simuni, 2017) calcium
645 homeostasis have been linked to dystonia and Parkinson disease, respectively.
646 A small pedigree (Figure 6) with BSP+ and Parkinsonism harboring variants in
647 *HS1BP3* and *GNA14* highlights the distinct possibility of oligogenic inheritance in BSP
648 and other anatomical distributions of dystonia. In particular, all of the exomes
649 sequenced in this study harbored more than one potentially pathogenic variant. Since
650 most of our pedigrees were small and moderate numbers of variants showed *in silico*
651 evidence of deleteriousness, we did not assess co-segregration for all of the identified
652 candidate variants. However, we determined that both *GNA14* and *HS1PB3* were

653 attractive candidate genes. Guanine nucleotide-binding protein subunit alpha-14
654 (encoded by *GNA14*) interacts with dynein, axonemal, light chain 4 (UniProt) which is
655 expressed at high levels in sperm and brain. *GNA14* appears to play a key role in the
656 genetic architecture underlying normal gray matter density (Chen et al., 2015) and a
657 *GNA14* deletion mutation has been reported in a patient with early-onset Alzheimer
658 disease (Lazarczyk et al., 2017). *HS1BP3* shows moderate expression in brain (The
659 Human Protein Atlas), and, in cerebellum, appears at highest levels in Purkinje cells
660 (Allen Brain Atlas). Multipoint linkage analysis in four large pedigrees with ET identified
661 a critical region between loci D2S2150 and D2S220 on Chr 2p which includes *HS1BP3*
662 (Higgins, Loveless, Jankovic, & Patel, 1998). The p.A265G HCLS1-binding protein 3
663 (HS1BP3) variant encoded by *HS1BP3* is in linkage disequilibrium with ET but is
664 unlikely to be causal since it is present at high frequency in the general population
665 (Shatunov et al., 2005). It remains unknown if other coding or non-coding variants in
666 *HS1BP3* are causally related to the pathogenesis of ET. HS1BP3 negatively regulates
667 autophagy (Holland et al., 2016), a cellular pathway closely tied to several
668 neurodegenerative disorders including PD (Nash, Schmukler, Trudler, Pinkas-
669 Kramarski, & Frenkel, 2017). In this regard, ET and PD may be related to adult-onset
670 dystonia through common genetics (De Rosa et al., 2016; Dubinsky, Gray, & Koller,
671 1993; Hedera et al., 2010; LeDoux et al., 2016; Louis et al., 2012; Straniero et al.,
672 2017).

673 Oligenic inheritance is caused by mutations in two or more proteins with a functional
674 relationship through direct interactions, membership in a pathway, or co-expression in a
675 specific cell type. Given that functional groups of genes tend to co-localize within

676 chromosomes (Thevenin, Ein-Dor, Ozery-Flato, & Shamir, 2014), the possibility of
677 oligogenic inheritance of variants found within a locus defined by linkage analysis
678 cannot be ignored. Our focused analyses of the DYT13 and DYT21 loci provide genes
679 and variants for co-segregation analysis in these previously detailed dystonia pedigrees
680 and suggest that digenic or higher-order oligogenic inheritance of variants within a
681 disease-associated locus may be causal in some pedigrees and isolated cases with
682 BSP. In this regard, co-segregating variants in *CIZ1* and *SETX* were linked to cervical
683 dystonia in a large American pedigree (Xiao et al., 2012).
684 BSP exerts important effects on health-related quality of life (Hall et al., 2006). Many
685 patients with BSP experience annoying dry eye symptoms and photophobia (Hallett,
686 Evinger, Jankovic, Stacy, & Workshop, 2008). Oral medications such as
687 anticholinergics and benzodiazepines are mildly beneficial in some subjects. Many
688 patients with BSP show moderate benefit from injections of botulinum toxin. However,
689 injections are expensive, painful and may be denied by third-party payers. Although
690 deep brain stimulation has been used to treat some individuals with BSP+ phenotypes,
691 responses have been mixed (Reese et al., 2011). Major advances in the treatment of
692 BSP demand a deeper understanding of its genetic etiopathogenesis. Our work
693 provides a platform for follow-up case-control analyses of identified variants, evaluation
694 of digenic and higher-order oliogenic etiologies for BSP (Deltas, 2017), and generation
695 of animal models to help assess the pathogenicity of identified variants. Future work
696 will demand attention to the effects of genetic background, oligogenic inheritance,
697 pleiotropy, confounds of phenocopies, and the limitations of WES.
698

699 **ACKNOWLEDGMENTS**

700 Utmost thanks go to the many families that participating in this study. M.S.L. was
701 supported by the Benign Essential Blepharospasm Research Foundation, Neuroscience
702 Institute at the University of Tennessee Health Science Center (UHTSC), UTHSC iRISE
703 Pilot Translational and Clinical Studies Program, Dorothy/Daniel Gerwin Parkinson
704 Research Fund, Department of Defense grant W81XWH-17-1-0062 and National
705 Institutes of Health (NIH) grants R01 NS082296, R21 GM118962, and R56 NS094965.
706 Z.K.W. was partially supported by the NIH/National Institute of Neurological Diseases
707 and Stroke (NINDS) P50 NS072187, NIH/National Institute of Aging (NIA) (primary) and
708 NIH/NINDS (secondary) 1U01AG045390-01A1, Mayo Clinic Center for Regenerative
709 Medicine, Mayo Clinic Center for Individualized Medicine, Mayo Clinic Neuroscience
710 Focused Research Team (Cecilia and Dan Carmichael Family Foundation, and the
711 James C. and Sarah K. Kennedy Fund for Neurodegenerative Disease Research at
712 Mayo Clinic in Florida), a gift from Carl Edward Bolch, Jr., and Susan Bass Bolch, The
713 Sol Goldman Charitable Trust, and Donald G. and Jodi P. Heeringa. At the University
714 of Tennessee Health Science Center, Vanisha Patel participated in Sanger sequencing
715 and quantitative PCR. At the Mayo Clinic Florida, Audrey Strongosky and Anne Martin
716 participated in the collection of blood samples and phenotypic information.

717

718 **DISCLOSURE STATEMENT**

719 The authors declare no conflict of interest.

720

721 **WEB RESOURCES**

722 1000 Genomes, http://www.1000genomes.org/

723 Allen Brain Atlas, http://www.brain-map.org/

724 BioGRID, https://thebiogrid.org/

725 BioGPS, http://biogps.org/

726 ExAC Browser, http://exac.broadinstitute.org/

727 CADD, http://cadd.gs.washington.edu/

728 Clustal Omega, https://www.ebi.ac.uk/Tools/msa/clustal0/

729 gnomAD, http://gnomad.broadinstitute.org/

730 MARRVEL, http://marrvel.org/

731 MutationTaster, http://www.mutationtaster.org/

732 NCBI, https://www.ncbi.nlm.nih.gov/

733 NHLBI Exome Sequencing Project (ESP) Exome Variant Server (EVS),

734 http://evs.gs.washington.edu/EVS/

735 OMIM, http://www.omim.org/

736 UniProt, http://www.uniprot.org/

737

References

Ahrenstorf, G., Low, H. Z., Kniesch, K., Ordonez, D., Meyer-Olson, D., Ahmad, F., . . . Witte, T. (2017). LILRA3 deletion is a genetic risk factor of HIV infection. *AIDS, 31*(1), 25-34. doi:10.1097/QAD.0000000000001304

Albanese, A., Bhatia, K., Bressman, S. B., Delong, M. R., Fahn, S., Fung, V. S., . . . Teller, J. K. (2013). Phenomenology and classification of dystonia: a consensus update. *Mov Disord, 28*(7), 863-873. doi:10.1002/mds.25475

Argasinska, J., Rana, A. A., Gilchrist, M. J., Lachani, K., Young, A., & Smith, J. C. (2009). Loss of REEP4 causes paralysis of the Xenopus embryo. *Int J Dev Biol, 53*(1), 37-43. doi:10.1387/ijdb.072542ja

Bentivoglio, A. R., Del Grosso, N., Albanese, A., Cassetta, E., Tonali, P., & Frontali, M. (1997). Non-DYT1 dystonia in a large Italian family. *J Neurol Neurosurg Psychiatry, 62*(4), 357-360.

Bressman, S. B., Sabatti, C., Raymond, D., de Leon, D., Klein, C., Kramer, P. L., . . . Risch, N. J. (2000). The DYT1 phenotype and guidelines for diagnostic testing. *Neurology, 54*(9), 1746-1752.

Cain, S. M., & Snutch, T. P. (2011). Voltage-gated calcium channels and disease. *Biofactors, 37*(3), 197-205. doi:10.1002/biof.158

Charlesworth, G., Angelova, P. R., Bartolome-Robledo, F., Ryten, M., Trabzuni, D., Stamelou, M., . . . Wood, N. W. (2015). Mutations in HPCA cause autosomal-recessive primary isolated dystonia. *Am J Hum Genet, 96*(4), 657-665. doi:10.1016/j.ajhg.2015.02.007

Chen, J., Calhoun, V. D., Arias-Vasquez, A., Zwiers, M. P., van Hulzen, K., Fernandez, G., . . . Liu, J. (2015). G-protein genomic association with normal variation in gray matter density. *Hum Brain Mapp, 36*(11), 4272-4286. doi:10.1002/hbm.22916

Conroy, J., McGettigan, P., Murphy, R., Webb, D., Murphy, S. M., McCoy, B., . . . Ennis, S. (2014). A novel locus for episodic ataxia:UBR4 the likely candidate. *Eur J Hum Genet, 22*(4), 505-510. doi:10.1038/ejhg.2013.173

Conte, A., Ferrazzano, G., Defazio, G., Fabbrini, G., Hallett, M., & Berardelli, A. (2017). Increased Blinking May Be a Precursor of Blepharospasm: A Longitudinal Study. *Mov Disord Clin Pract, 4*(5), 733-736. doi:10.1002/mdc3.12499

De Rosa, A., Pellegrino, T., Pappata, S., Lieto, M., Bonifati, V., Palma, V., . . . De Michele, G. (2016). Non-motor symptoms and cardiac innervation in SYNJ1-related parkinsonism. *Parkinsonism Relat Disord, 23*, 102-105. doi:10.1016/j.parkreldis.2015.12.006

Defazio, G., Abbruzzese, G., Livrea, P., & Berardelli, A. (2004). Epidemiology of primary dystonia. *Lancet Neurol, 3*(11), 673-678. doi:10.1016/S1474-4422(04)00907-X

Defazio, G., Berardelli, A., & Hallett, M. (2007). Do primary adult-onset focal dystonias share aetiological factors? *Brain, 130*(Pt 5), 1183-1193. doi:10.1093/brain/awl355

Defazio, G., Hallett, M., Jinnah, H. A., & Berardelli, A. (2013). Development and validation of a clinical guideline for diagnosing blepharospasm. *Neurology, 81*(3), 236-240. doi:10.1212/WNL.0b013e31829bfdf6

Defazio, G., Hallett, M., Jinnah, H. A., Stebbins, G. T., Gigante, A. F., Ferrazzano, G., . . . Berardelli, A. (2015). Development and validation of a clinical scale for rating the severity of blepharospasm. *Mov Disord, 30*(4), 525-530. doi:10.1002/mds.26156

Defazio, G., Livrea, P., Guanti, G., Lepore, V., & Ferrari, E. (1993). Genetic contribution to idiopathic adult-onset blepharospasm and cranial-cervical dystonia. *Eur Neurol, 33*(5), 345-350.

Defazio, G., Martino, D., Aniello, M. S., Masi, G., Abbruzzese, G., Lamberti, S., . . . Berardelli, A. (2006). A family study on primary blepharospasm. *J Neurol Neurosurg Psychiatry, 77*(2), 252-254. doi:10.1136/jnnp.2005.068007

Defazio, G., Martino, D., Aniello, M. S., Masi, G., Gigante, A., Bhatia, K., . . . Berardelli, A. (2006). Planning genetic studies on primary adult-onset dystonia: sample size estimates based on examination of first-degree relatives. *J Neurol Sci, 251*(1-2), 29-34. doi:10.1016/j.jns.2006.08.009

Deltas, C. (2017). Digenic inheritance and genetic modifiers. *Clin Genet*. doi:10.1111/cge.13150

Dong, C., Wei, P., Jian, X., Gibbs, R., Boerwinkle, E., Wang, K., & Liu, X. (2015). Comparison and integration of deleteriousness prediction methods for nonsynonymous SNVs in whole exome sequencing studies. *Hum Mol Genet, 24*(8), 2125-2137. doi:10.1093/hmg/ddu733

Dorboz, I., Coutelier, M., Bertrand, A. T., Caberg, J. H., Elmaleh-Berges, M., Laine, J., . . . Servais, L. (2014). Severe dystonia, cerebellar atrophy, and cardiomyopathy likely caused by a missense mutation in TOR1AIP1. *Orphanet J Rare Dis, 9*, 174. doi:10.1186/s13023-014-0174-9

Du, Y., Su, Y., He, J., Yang, Y., Shi, Y., Cui, Y., . . . Li, Z. (2015). Impact of the leucocyte immunoglobulin-like receptor A3 (LILRA3) on susceptibility and subphenotypes of systemic lupus erythematosus and Sjogren's syndrome. *Ann Rheum Dis, 74*(11), 2070-2075. doi:10.1136/annrheumdis-2013-204441

Dubinsky, R. M., Gray, C. S., & Koller, W. C. (1993). Essential tremor and dystonia. *Neurology, 43*(11), 2382-2384.

Estrada-Cuzcano, A., Martin, S., Chamova, T., Synofzik, M., Timmann, D., Holemans, T., . . . Schule, R. (2017). Loss-of-function mutations in the ATP13A2/PARK9 gene cause complicated hereditary spastic paraplegia (SPG78). *Brain, 140*(2), 287-305. doi:10.1093/brain/aww307

Fernandez, H. H., Jankovic, J., Holds, J. B., Lin, D., Burns, J., Verma, A., . . . Pappert, E. J. (2014). Observational Study of IncobotulinumtoxinA for Cervical Dystonia or Blepharospasm (XCiDaBLE): Interim Results for the First 170 Subjects with Blepharospasm. *Tremor Other Hyperkinet Mov (N Y), 4*, 238. doi:10.7916/D8MK6B1B

Foo, J. N., Tan, L. C., Irwan, I. D., Au, W. L., Low, H. Q., Prakash, K. M., . . . Tan, E. K. (2017). Genome-wide association study of Parkinson's disease in East Asians. *Hum Mol Genet, 26*(1), 226-232. doi:10.1093/hmg/ddw379

Forsgren, L., Holmgren, G., Almay, B. G., & Drugge, U. (1988). Autosomal dominant torsion dystonia in a Swedish family. *Adv Neurol, 50*, 83-92.

Granneman, S., Gallagher, J. E., Vogelzangs, J., Horstman, W., van Venrooij, W. J., Baserga, S. J., & Pruijn, G. J. (2003). The human Imp3 and Imp4 proteins form a ternary complex with hMpp10, which only interacts with the U3 snoRNA in 60-80S ribonucleoprotein complexes. *Nucleic Acids Res, 31*(7), 1877-1887.

Hall, T. A., McGwin, G., Jr., Searcey, K., Xie, A., Hupp, S. L., Owsley, C., & Kline, L. B. (2006). Health-related quality of life and psychosocial characteristics of patients

830 with benign essential blepharospasm. *Arch Ophthalmol, 124*(1), 116-119.
831 doi:10.1001/archopht.124.1.116
832 Hallett, M., Evinger, C., Jankovic, J., Stacy, M., & Workshop, B. I. (2008). Update on
833 blepharospasm: report from the BEBRF International Workshop. *Neurology,*
834 *71*(16), 1275-1282. doi:10.1212/01.wnl.0000327601.46315.85
835 Hedera, P., Phibbs, F. T., Fang, J. Y., Cooper, M. K., Charles, P. D., & Davis, T. L.
836 (2010). Clustering of dystonia in some pedigrees with autosomal dominant
837 essential tremor suggests the existence of a distinct subtype of essential tremor.
838 *BMC Neurol, 10*, 66. doi:10.1186/1471-2377-10-66
839 Higgins, J. J., Lombardi, R. Q., Pucilowska, J., Jankovic, J., Tan, E. K., & Rooney, J. P.
840 (2005). A variant in the HS1-BP3 gene is associated with familial essential
841 tremor. *Neurology, 64*(3), 417-421. doi:10.1212/01.WNL.0000153481.30222.38
842 Higgins, J. J., Loveless, J. M., Jankovic, J., & Patel, P. I. (1998). Evidence that a gene
843 for essential tremor maps to chromosome 2p in four families. *Mov Disord, 13*(6),
844 972-977. doi:10.1002/mds.870130621
845 Holland, P., Knaevelsrud, H., Soreng, K., Mathai, B. J., Lystad, A. H., Pankiv, S., . . .
846 Simonsen, A. (2016). HS1BP3 negatively regulates autophagy by modulation of
847 phosphatidic acid levels. *Nat Commun, 7*, 13889. doi:10.1038/ncomms13889
848 Ioannidis, N. M., Rothstein, J. H., Pejaver, V., Middha, S., McDonnell, S. K., Baheti, S., .
849 . . Sieh, W. (2016). REVEL: An Ensemble Method for Predicting the
850 Pathogenicity of Rare Missense Variants. *Am J Hum Genet, 99*(4), 877-885.
851 doi:10.1016/j.ajhg.2016.08.016
852 Jian, X., Boerwinkle, E., & Liu, X. (2014). In silico prediction of splice-altering single
853 nucleotide variants in the human genome. *Nucleic Acids Res, 42*(22), 13534-
854 13544. doi:10.1093/nar/gku1206
855 Kawaji, H., Kasukawa, T., Forrest, A., Carninci, P., & Hayashizaki, Y. (2017). The
856 FANTOM5 collection, a data series underpinning mammalian transcriptome
857 atlases in diverse cell types. *Sci Data, 4*, 170113. doi:10.1038/sdata.2017.113
858 Kawalia, S. B., Raschka, T., Naz, M., de Matos Simoes, R., Senger, P., & Hofmann-
859 Apitius, M. (2017). Analytical Strategy to Prioritize Alzheimer's Disease
860 Candidate Genes in Gene Regulatory Networks Using Public Expression Data. *J*
861 *Alzheimers Dis, 59*(4), 1237-1254. doi:10.3233/JAD-170011
862 Kircher, M., Witten, D. M., Jain, P., O'Roak, B. J., Cooper, G. M., & Shendure, J. (2014).
863 A general framework for estimating the relative pathogenicity of human genetic
864 variants. *Nat Genet, 46*(3), 310-315. doi:10.1038/ng.2892
865 Klebe, S., Stevanin, G., & Depienne, C. (2015). Clinical and genetic heterogeneity in
866 hereditary spastic paraplegias: from SPG1 to SPG72 and still counting. *Rev*
867 *Neurol (Paris), 171*(6-7), 505-530. doi:10.1016/j.neurol.2015.02.017
868 Korosec, B., Glavac, D., Volavsek, M., & Ravnik-Glavac, M. (2009). ATP2A3 gene is
869 involved in cancer susceptibility. *Cancer Genet Cytogenet, 188*(2), 88-94.
870 doi:10.1016/j.cancergencyto.2008.10.007
871 Kuo, P. H., Gan, S. R., Wang, J., Lo, R. Y., Figueroa, K. P., Tomishon, D., . . . Kuo, S.
872 H. (2017). Dystonia and ataxia progression in spinocerebellar ataxias.
873 *Parkinsonism Relat Disord*. doi:10.1016/j.parkreldis.2017.10.007

874 Laudermilch, E., Tsai, P. L., Graham, M., Turner, E., Zhao, C., & Schlieker, C. (2016).
875 Dissecting Torsin/cofactor function at the nuclear envelope: a genetic study. *Mol*
876 *Biol Cell, 27*(25), 3964-3971. doi:10.1091/mbc.E16-07-0511
877 Lazarczyk, M. J., Haller, S., Savioz, A., Gimelli, S., Bena, F., & Giannakopoulos, P.
878 (2017). Heterozygous Deletion of Chorein Exons 70-73 and GNA14 Exons 3-7 in
879 a Brazilian Patient Presenting With Probable Tau-Negative Early-Onset
880 Alzheimer Disease. *Alzheimer Dis Assoc Disord, 31*(1), 82-85.
881 doi:10.1097/WAD.0000000000000185
882 LeDoux, M. S. (2009). Meige syndrome: what's in a name? *Parkinsonism Relat Disord,*
883 *15*(7), 483-489. doi:10.1016/j.parkreldis.2009.04.006
884 LeDoux, M. S. (2011). Animal models of dystonia: Lessons from a mutant rat. *Neurobiol*
885 *Dis, 42*(2), 152-161. doi:10.1016/j.nbd.2010.11.006
886 LeDoux, M. S. (2012). The genetics of dystonias. *Adv Genet, 79*, 35-85.
887 doi:10.1016/B978-0-12-394395-8.00002-5
888 LeDoux, M. S., Vemula, S. R., Xiao, J., Thompson, M. M., Perlmutter, J. S., Wright, L.
889 J., . . . Stover, N. P. (2016). Clinical and genetic features of cervical dystonia in a
890 large multicenter cohort. *Neurol Genet, 2*(3), e69.
891 doi:10.1212/NXG.0000000000000069
892 LeDoux, M. S., Xiao, J., Rudzinska, M., Bastian, R. W., Wszolek, Z. K., Van Gerpen, J.
893 A., . . . Zhao, Y. (2012). Genotype-phenotype correlations in THAP1 dystonia:
894 molecular foundations and description of new cases. *Parkinsonism Relat Disord,*
895 *18*(5), 414-425. doi:10.1016/j.parkreldis.2012.02.001
896 Lek, M., Karczewski, K. J., Minikel, E. V., Samocha, K. E., Banks, E., Fennell, T., . . .
897 Exome Aggregation, C. (2016). Analysis of protein-coding genetic variation in
898 60,706 humans. *Nature, 536*(7616), 285-291. doi:10.1038/nature19057
899 Lesage, S., Drouet, V., Majounie, E., Deramecourt, V., Jacoupy, M., Nicolas, A., . . .
900 International Parkinson's Disease Genomics, C. (2016). Loss of VPS13C
901 Function in Autosomal-Recessive Parkinsonism Causes Mitochondrial
902 Dysfunction and Increases PINK1/Parkin-Dependent Mitophagy. *Am J Hum*
903 *Genet, 98*(3), 500-513. doi:10.1016/j.ajhg.2016.01.014
904 Leube, B., Kessler, K. R., Goecke, T., Auburger, G., & Benecke, R. (1997). Frequency
905 of familial inheritance among 488 index patients with idiopathic focal dystonia
906 and clinical variability in a large family. *Mov Disord, 12*(6), 1000-1006.
907 doi:10.1002/mds.870120625
908 Lim, Y. H., Bacchiocchi, A., Qiu, J., Straub, R., Bruckner, A., Bercovitch, L., . . . Choate,
909 K. A. (2016). GNA14 Somatic Mutation Causes Congenital and Sporadic
910 Vascular Tumors by MAPK Activation. *Am J Hum Genet, 99*(2), 443-450.
911 doi:10.1016/j.ajhg.2016.06.010
912 Liu, X., Jian, X., & Boerwinkle, E. (2011). dbNSFP: a lightweight database of human
913 nonsynonymous SNPs and their functional predictions. *Hum Mutat, 32*(8), 894-
914 899. doi:10.1002/humu.21517
915 Liu, X., Wu, C., Li, C., & Boerwinkle, E. (2016). dbNSFP v3.0: A One-Stop Database of
916 Functional Predictions and Annotations for Human Nonsynonymous and Splice-
917 Site SNVs. *Hum Mutat, 37*(3), 235-241. doi:10.1002/humu.22932
918 Louis, E. D., Hernandez, N., Alcalay, R. N., Tirri, D. J., Ottman, R., & Clark, L. N.
919 (2012). Prevalence and features of unreported dystonia in a family study of

"pure" essential tremor. *Parkinsonism Relat Disord*. doi:10.1016/j.parkreldis.2012.09.015

Lubbe, S. J., Escott-Price, V., Gibbs, J. R., Nalls, M. A., Bras, J., Price, T. R., . . . for International Parkinson's Disease Genomics, C. (2016). Additional rare variant analysis in Parkinson's disease cases with and without known pathogenic mutations: evidence for oligogenic inheritance. *Hum Mol Genet, 25*(24), 5483-5489. doi:10.1093/hmg/ddw348

Matak, P., Matak, A., Moustafa, S., Aryal, D. K., Benner, E. J., Wetsel, W., & Andrews, N. C. (2016). Disrupted iron homeostasis causes dopaminergic neurodegeneration in mice. *Proc Natl Acad Sci U S A, 113*(13), 3428-3435. doi:10.1073/pnas.1519473113

Miles, L. B., Darido, C., Kaslin, J., Heath, J. K., Jane, S. M., & Dworkin, S. (2017). Mis-expression of grainyhead-like transcription factors in zebrafish leads to defects in enveloping layer (EVL) integrity, cellular morphogenesis and axial extension. *Sci Rep, 7*(1), 17607. doi:10.1038/s41598-017-17898-7

Naik, S., Pohl, K., Malik, M., Siddiqui, A., & Josifova, D. (2011). Early-onset cerebellar atrophy associated with mutation in the CACNA1A gene. *Pediatr Neurol, 45*(5), 328-330. doi:10.1016/j.pediatrneurol.2011.08.002

Nash, Y., Schmukler, E., Trudler, D., Pinkas-Kramarski, R., & Frenkel, D. (2017). DJ-1 deficiency impairs autophagy and reduces alpha-synuclein phagocytosis by microglia. *J Neurochem, 143*(5), 584-594. doi:10.1111/jnc.14222

Norgren, N., Mattson, E., Forsgren, L., & Holmberg, M. (2011). A high-penetrance form of late-onset torsion dystonia maps to a novel locus (DYT21) on chromosome 2q14.3-q21.3. *Neurogenetics, 12*(2), 137-143. doi:10.1007/s10048-011-0274-9

O'Riordan, S., Raymond, D., Lynch, T., Saunders-Pullman, R., Bressman, S. B., Daly, L., & Hutchinson, M. (2004). Age at onset as a factor in determining the phenotype of primary torsion dystonia. *Neurology, 63*(8), 1423-1426.

Ophoff, R. A., Terwindt, G. M., Vergouwe, M. N., van Eijk, R., Oefner, P. J., Hoffman, S. M., . . . Frants, R. R. (1996). Familial hemiplegic migraine and episodic ataxia type-2 are caused by mutations in the Ca2+ channel gene CACNL1A4. *Cell, 87*(3), 543-552.

Ozelius, L. J., Hewett, J. W., Page, C. E., Bressman, S. B., Kramer, P. L., Shalish, C., . . . Breakefield, X. O. (1997). The early-onset torsion dystonia gene (DYT1) encodes an ATP-binding protein. *Nat Genet, 17*(1), 40-48. doi:10.1038/ng0997-40

Ozelius, L. J., Page, C. E., Klein, C., Hewett, J. W., Mineta, M., Leung, J., . . . Breakefield, X. O. (1999). The TOR1A (DYT1) gene family and its role in early onset torsion dystonia. *Genomics, 62*(3), 377-384. doi:10.1006/geno.1999.6039

Parkinson, N. J., Olsson, C. L., Hallows, J. L., McKee-Johnson, J., Keogh, B. P., Noben-Trauth, K., . . . Tempel, B. L. (2001). Mutant beta-spectrin 4 causes auditory and motor neuropathies in quivering mice. *Nat Genet, 29*(1), 61-65. doi:10.1038/ng710

Pirio Richardson, S., Wegele, A. R., Skipper, B., Deligtisch, A., Jinnah, H. A., & Dystonia Coalition, I. (2017). Dystonia treatment: Patterns of medication use in an international cohort. *Neurology, 88*(6), 543-550. doi:10.1212/WNL.0000000000003596

966 Prudente, C. N., Pardo, C. A., Xiao, J., Hanfelt, J., Hess, E. J., Ledoux, M. S., & Jinnah,
967 H. A. (2013). Neuropathology of cervical dystonia. *Exp Neurol, 241*, 95-104.
968 doi:10.1016/j.expneurol.2012.11.019
969 Qin, J., Jones, R. C., & Ramakrishnan, R. (2008). Studying copy number variations
970 using a nanofluidic platform. *Nucleic Acids Res, 36*(18), e116.
971 doi:10.1093/nar/gkn518
972 Ramirez, A., Heimbach, A., Grundemann, J., Stiller, B., Hampshire, D., Cid, L. P., . . .
973 Kubisch, C. (2006). Hereditary parkinsonism with dementia is caused by
974 mutations in ATP13A2, encoding a lysosomal type 5 P-type ATPase. *Nat Genet,*
975 *38*(10), 1184-1191. doi:10.1038/ng1884
976 Reese, R., Gruber, D., Schoenecker, T., Bazner, H., Blahak, C., Capelle, H. H., . . .
977 Krauss, J. K. (2011). Long-term clinical outcome in meige syndrome treated with
978 internal pallidum deep brain stimulation. *Mov Disord, 26*(4), 691-698.
979 doi:10.1002/mds.23549
980 Schlaitz, A. L., Thompson, J., Wong, C. C., Yates, J. R., 3rd, & Heald, R. (2013).
981 REEP3/4 ensure endoplasmic reticulum clearance from metaphase chromatin
982 and proper nuclear envelope architecture. *Dev Cell, 26*(3), 315-323.
983 doi:10.1016/j.devcel.2013.06.016
984 Schwarz, J. M., Cooper, D. N., Schuelke, M., & Seelow, D. (2014). MutationTaster2:
985 mutation prediction for the deep-sequencing age. *Nat Methods, 11*(4), 361-362.
986 doi:10.1038/nmeth.2890
987 Schwarz, J. M., Rodelsperger, C., Schuelke, M., & Seelow, D. (2010). MutationTaster
988 evaluates disease-causing potential of sequence alterations. *Nat Methods, 7*(8),
989 575-576. doi:10.1038/nmeth0810-575
990 Sethi, K. D., & Jankovic, J. (2002). Dystonia in spinocerebellar ataxia type 6. *Mov*
991 *Disord, 17*(1), 150-153.
992 Shatunov, A., Jankovic, J., Elble, R., Sambuughin, N., Singleton, A., Hallett, M., &
993 Goldfarb, L. (2005). A variant in the HS1-BP3 gene is associated with familial
994 essential tremor. *Neurology, 65*(12), 1995; author reply 1995.
995 doi:10.1212/01.wnl.0000200984.10076.e5
996 Shin, M., Douglass, L. M., Milunsky, J. M., & Rosman, N. P. (2016). The Genetics of
997 Benign Paroxysmal Torticollis of Infancy: Is There an Association With Mutations
998 in the CACNA1A Gene? *J Child Neurol, 31*(8), 1057-1061.
999 doi:10.1177/0883073816636226
1000 Spacey, S. (1993). Episodic Ataxia Type 2. In M. P. Adam, H. H. Ardinger, R. A. Pagon,
1001 S. E. Wallace, L. J. H. Bean, K. Stephens, & A. Amemiya (Eds.),
1002 *GeneReviews((R))*. Seattle (WA).
1003 Spacey, S. D., Materek, L. A., Szczygielski, B. I., & Bird, T. D. (2005). Two novel
1004 CACNA1A gene mutations associated with episodic ataxia type 2 and interictal
1005 dystonia. *Arch Neurol, 62*(2), 314-316. doi:10.1001/archneur.62.2.314
1006 Stojanovic, M., Cvetkovic, D., & Kostic, V. S. (1995). A genetic study of idiopathic focal
1007 dystonias. *J Neurol, 242*(8), 508-511.
1008 Straniero, L., Guella, I., Cilia, R., Parkkinen, L., Rimoldi, V., Young, A., . . . Duga, S.
1009 (2017). DNAJC12 and dopa-responsive nonprogressive parkinsonism. *Ann*
1010 *Neurol, 82*(4), 640-646. doi:10.1002/ana.25048

1011 Surmeier, D. J., Halliday, G. M., & Simuni, T. (2017). Calcium, mitochondrial dysfunction
1012 and slowing the progression of Parkinson's disease. *Exp Neurol, 298*(Pt B), 202-
1013 209. doi:10.1016/j.expneurol.2017.08.001
1014 Talevich, E., Shain, A. H., Botton, T., & Bastian, B. C. (2016). CNVkit: Genome-Wide
1015 Copy Number Detection and Visualization from Targeted DNA Sequencing.
1016 *PLoS Comput Biol, 12*(4), e1004873. doi:10.1371/journal.pcbi.1004873
1017 Thevenin, A., Ein-Dor, L., Ozery-Flato, M., & Shamir, R. (2014). Functional gene groups
1018 are concentrated within chromosomes, among chromosomes and in the nuclear
1019 space of the human genome. *Nucleic Acids Res, 42*(15), 9854-9861.
1020 doi:10.1093/nar/gku667
1021 Thomsen, L. L., Oestergaard, E., Bjornsson, A., Stefansson, H., Fasquel, A. C.,
1022 Gulcher, J., . . . Olesen, J. (2008). Screen for CACNA1A and ATP1A2 mutations
1023 in sporadic hemiplegic migraine patients. *Cephalalgia, 28*(9), 914-921.
1024 doi:10.1111/j.1468-2982.2008.01599.x
1025 Tzingounis, A. V., Kobayashi, M., Takamatsu, K., & Nicoll, R. A. (2007). Hippocalcin
1026 gates the calcium activation of the slow afterhyperpolarization in hippocampal
1027 pyramidal cells. *Neuron, 53*(4), 487-493. doi:10.1016/j.neuron.2007.01.011
1028 Valente, E. M., Bentivoglio, A. R., Cassetta, E., Dixon, P. H., Davis, M. B., Ferraris, A., .
1029 . . Albanese, A. (2001). DYT13, a novel primary torsion dystonia locus, maps to
1030 chromosome 1p36.13--36.32 in an Italian family with cranial-cervical or upper
1031 limb onset. *Ann Neurol, 49*(3), 362-366.
1032 van Gassen, K. L., van der Heijden, C. D., de Bot, S. T., den Dunnen, W. F., van den
1033 Berg, L. H., Verschuuren-Bemelmans, C. C., . . . van de Warrenburg, B. P.
1034 (2012). Genotype-phenotype correlations in spastic paraplegia type 7: a study in
1035 a large Dutch cohort. *Brain, 135*(Pt 10), 2994-3004. doi:10.1093/brain/aws224
1036 Vemula, S. R., Puschmann, A., Xiao, J., Zhao, Y., Rudzinska, M., Frei, K. P., . . .
1037 LeDoux, M. S. (2013). Role of Galpha(olf) in familial and sporadic adult-onset
1038 primary dystonia. *Hum Mol Genet, 22*(12), 2510-2519. doi:10.1093/hmg/ddt102
1039 Vemula, S. R., Xiao, J., Zhao, Y., Bastian, R. W., Perlmutter, J. S., Racette, B. A., . . .
1040 LeDoux, M. S. (2014). A rare sequence variant in intron 1 of THAP1 is
1041 associated with primary dystonia. *Mol Genet Genomic Med, 2*(3), 261-272.
1042 doi:10.1002/mgg3.67
1043 Waddy, H. M., Fletcher, N. A., Harding, A. E., & Marsden, C. D. (1991). A genetic study
1044 of idiopathic focal dystonias. *Ann Neurol, 29*(3), 320-324.
1045 doi:10.1002/ana.410290315
1046 Waln, O., & LeDoux, M. S. (2011). Blepharospasm plus Cervical Dystonia with
1047 Predominant Anterocollis: A Distinctive Subphenotype of Segmental
1048 Craniocervical Dystonia? *Tremor Other Hyperkinet Mov (N Y), 2011*(1).
1049 Weiss, E. M., Hershey, T., Karimi, M., Racette, B., Tabbal, S. D., Mink, J. W., . . .
1050 Perlmutter, J. S. (2006). Relative risk of spread of symptoms among the focal
1051 onset primary dystonias. *Mov Disord, 21*(8), 1175-1181. doi:10.1002/mds.20919
1052 Xiao, J., Bastian, R. W., Perlmutter, J. S., Racette, B. A., Tabbal, S. D., Karimi, M., . . .
1053 LeDoux, M. S. (2009). High-throughput mutational analysis of TOR1A in primary
1054 dystonia. *BMC Med Genet, 10*, 24. doi:10.1186/1471-2350-10-24

1055 Xiao, J., Thompson, M. M., Vemula, S. R., & LeDoux, M. S. (2016). Blepharospasm in a
1056 multiplex African-American pedigree. *J Neurol Sci, 362*, 299-303.
1057 doi:10.1016/j.jns.2016.02.003
1058 Xiao, J., Uitti, R. J., Zhao, Y., Vemula, S. R., Perlmutter, J. S., Wszolek, Z. K., . . .
1059 LeDoux, M. S. (2012). Mutations in CIZ1 cause adult onset primary cervical
1060 dystonia. *Ann Neurol, 71*(4), 458-469. doi:10.1002/ana.23547
1061 Xiao, J., Zhao, Y., Bastian, R. W., Perlmutter, J. S., Racette, B. A., Tabbal, S. D., . . .
1062 LeDoux, M. S. (2011). The c.-237_236GA>TT THAP1 sequence variant does not
1063 increase risk for primary dystonia. *Mov Disord, 26*(3), 549-552.
1064 doi:10.1002/mds.23551
1065 Xiao, J., Zhao, Y., Bastian, R. W., Perlmutter, J. S., Racette, B. A., Tabbal, S. D., . . .
1066 LeDoux, M. S. (2010). Novel THAP1 sequence variants in primary dystonia.
1067 *Neurology, 74*(3), 229-238. doi:10.1212/WNL.0b013e3181ca00ca
1068 Zhuchenko, O., Bailey, J., Bonnen, P., Ashizawa, T., Stockton, D. W., Amos, C., . . .
1069 Lee, C. C. (1997). Autosomal dominant cerebellar ataxia (SCA6) associated with
1070 small polyglutamine expansions in the alpha 1A-voltage-dependent calcium
1071 channel. *Nat Genet, 15*(1), 62-69. doi:10.1038/ng0197-62

1072

1073 **Figure Legends**

1074 **Figure 1. BSP and BSP+ Pedigrees**

1075 Pedigrees with two or more affected individuals. Arrows, probands. Arrowheads, other
1076 family members analyzed with WES. White symbol, unaffected. Black symbols, BSP,
1077 BSP+ or other anatomical distribution of dystonia. Grey symbols, possibly affected.

1078

1079 **Figure 2. Flow Chart for WES Data Analysis**

1080 Analysis of exomes sequenced by BGI and Otogenetics. Otogenetics (Illumina) reads
1081 were mapped in house. BGI did not provide raw read data.

1082

1083 **Figure 3. *CACNA1A* INDEL Identified in a Multigenerational Pedigree with BSP**

1084 (A) Family NG0362 with BSP. Three affected (I-1, II-2 and III-1) individuals were
1085 selected for WES. +/+, wild-type. +/-, heterozygous for *CACNA1A*
1086 c.7261_7262delinsGT.
1087 (B) Electropherograms of unaffected family member (II-3) and subject with BSP (II-2).
1088 (C) Multiple sequence alignment shows evolutionary conservation of Pro2421 among
1089 mammals.
1090 (D) Location of disease-associated variants in the α-1A subunit of P/Q type, voltage-
1091 dependent, calcium channels: (1) Thr666Met variant linked to familial hemiplegic
1092 migraine and early-onset cerebellar atrophy (Naik et al., 2011; Ophoff et al., 1996), (2)
1093 variant (c.3772delC) predicted to cause a frameshift and truncated protein or, more
1094 likely, nonsense-mediated decay in a man with interictal BSP and episodic ataxia type 2
1095 (S. D. Spacey et al., 2005), (3), splice-site variant associated with episodic ataxia type 2
1096 (Ophoff et al., 1996), (4) Ile1811Leu variant associated with familial hemiplegic migraine

1097 (Ophoff et al., 1996), (5), Glu2080Lys variant linked to sporadic hemiplegic migraine
1098 (Thomsen et al., 2008), (6), CAG expansion associated with spinocerebellar ataxia type
1099 6 (SCA6) and dystonia (Kuo et al., 2017; Sethi & Jankovic, 2002; Zhuchenko et al.,
1100 1997), (7) Pro2421Val variant associated with BSP in our multigenerational pedigree,
1101 (8), Pro2479Leu associated with sporadic hemiplegic migraine (Thomsen et al., 2008),
1102 and (9) His2481Gln associated with sporadic hemiplegic migraine (Thomsen et al.,
1103 2008).
1104
1105 **Figure 4. *REEP4* Variant in African-American Pedigree with BSP+ and BSP**
1106 (A) Family 10908 with BSP+ and BSP. Two affected (II-3 and III-9) individuals were
1107 selected for WES. +/+, wild-type. +/-, heterozygous for *REEP4* c.109C>T.
1108 (B) Electropherograms of unaffected family member (II-2) and subject with BSP+ (II-3).
1109 (C) Multiple sequence alignment shows evolutionary conservation of Arg37 among
1110 vertebrates.
1111
1112 **Figure 5. *TOR2A* and *ATP2A3* Variants in Multigenerational Pedigrees with BSP**
1113 (A) Family NG0369 with BSP. Three affected (II-2, III-2 and III-6) individuals were
1114 selected for WES. +/+, wild-type. +/-, heterozygous for *TOR2A* c.568C>T.
1115 (B) Electropherograms of unaffected family member (II-6) and subject with BSP (II-2).
1116 (C) Multiple sequence alignment shows evolutionary conservation of Arg190 among
1117 vertebrates.
1118 (D) Discordant pedigree NG1072 with BSP, cervical dystonia, and arm dystonia. Two
1119 affected individuals were selected for WES (II-2, IV-2). +/+, wild-type. +/-, heterozygous

1120 for *ATP23* c.1966C>T. White symbol, unaffected. Black symbol, BSP, BSP+ or other
1121 anatomical distribution of dystonia. Grey symbol, possibly affected.
1122 (E) Electropherograms of unaffected family member (II-4) and subject with BSP (II-2).
1123 (F) Multiple sequence alignment shows evolutionary conservation of Arg656 among
1124 vertebrates.
1125

1126 **Figure 6. *GNA14* and *HS1BP3* Variants in Father and Son with BSP+**
1127 (A) Pedigree 10043. The proband has BSP+ and levodopa-responsive Parkinsonism.
1128 His father had BSP+ and both were selected for WES. +/+, wild-type. +/-, heterozygous
1129 for variants in *GNA14* and *HS1BP3*.
1130 (B) Electropherograms of unaffected family member (II-1) and proband (II-2) show
1131 *GNA14* variant.
1132 (C) Multiple sequence alignment shows evolutionary conservation of Thr330 among
1133 vertebrates.
1134 (D) Electropherograms of unaffected family member (II-1) and proband (II-2) show
1135 *HS1BP3* variant.
1136 (F) Multiple sequence alignment shows evolutionary conservation of Gly32 among
1137 vertebrates.
1138

1139 **Figure 7. *DHAH17* Variants in Pedigree and Isolated Subject with BSP**
1140 (A) Pedigree 45263 with BSP. +/+, wild-type. +/-, heterozygous for variant in *DNAH17*.
1141 (B) Electropherogram of proband (II-2) showing *DNAH17* variant.

1142 (C) Multiple sequence alignment shows evolutionary conservation of Pro3158 among
1143 vertebrates.
1144 (D) Electropherogram of subject 10076 showing c.13295G>A variant.
1145 (F) Multiple sequence alignment shows evolutionary conservation of Arg4432 among
1146 vertebrates.
1147

Table 1. BSP and BSP+ Subjects Examined with WES

Subject	Age	Age of Onset	Sex	Ethnicity	BSP Family History	Anatomical Distribution	Select candidate genes
10012	77	60	F	Caucasian	No	segmental dystonia (BSP, oromandibular, lower face, cervical)	*KCNH4, CHRNA7, SPTBN4, ATP13A2*
10014	70	47	F	Caucasian	No	segmental dystonia (BSP, oromandibular, lower face)	*KCNG4, PLP1, KCNS1, ACLY, VPS13C*
10035	67	55	F	Caucasian	No	segmental dystonia (BSP, oromandibular, lower face, cervical)	*TRPV4, TBP, IMP4, UBXN4*
10036	69	66	F	Caucasian	No	segmental dystonia (BSP, cervical)	*HK1, PRUNE2, NUMBL, MRPL15*
10043-I-1	83	57	M	Caucasian	Yes	segmental dystonia (BSP, oromandibular, lower face, cervical)	*GNA14, HS1BP3, NEFH, RWDD2A*
10043-II-2	51	45	M	Caucasian	Yes	segmental dystonia (BSP, pharyngeal, laryngeal, cervical), Parkinsonism	*GNA14. HS1BP3, NEFH, RWDD2A*
10064	60	47	M	Caucasian	Yes	segmental dystonia (BSP, oromandibular, lower face, cervical)	*HECW2, CDH4, RABL2B, AP4B1, SCN3A*
10076	62	61	F	Caucasian	No	segmental dystonia (BSP, cervical)	*CAPN11, REEP2, MYO1B, DNAH17, ATP13A2*
10178	59	20	M	Caucasian	Yes	BSP	*ZZEF1, KCNA5, MUYOD1, MRPL15*
10193	77	69	F	Caucasian	Yes	BSP	*IGSF21, MYOD1*
10274-II-3	56	45	M	AA	Yes	segmental dystonia (BSP, cervical)	*TRPV4, WDFY3, ZFYVE9*
10274-II-6	50	50	F	AA	Yes	BSP	*TRPV4, WDFY3, ZFYVE9*
10455	58	48	F	Caucasian	Yes	segmental dystonia (BSP, oromandibular, lower face, cervical)	*CADPS, SNPH, ATP2B1, SLC12A2, CAPN11, VSP13DC, SPTBN4, BTNL3*
10908-II-3	66	48	M	AA	Yes	segmental dystonia (BSP, oromandibular, lower face, cervical)	*REEP4*
10908-III-9	33	30	M	AA	Yes	BSP	*REEP4*
25056	70	59	F	Caucasian	Yes	segmental dystonia (BSP, oromandibular, lower face, arm tremor)	*ABCA2, MYT1L*
25069	61	56	M	Caucasian	Yes	BSP (with arm tremor)	*LRP1B, PCDHGA3, LAMA1, UNC13B, ATP13A2*
25215	57	54	F	Caucasian	Yes	BSP (with arm tremor)	*AGAP1, EPS15L1, SCN1A, UNC13B, TOP3B*
45263	78	77	M	Caucasian	Yes	BSP	*INO80, DNAH17*
85020	66	50	F	Caucasian	Yes	BSP	*LRP1, GCH1, DDHD2, UNK*
NG0362-II-2	57	39	M	Caucasian	Yes	BSP	*CACNA1A*
NG0362-I-1	76	67	M	Caucasian	Yes	BSP	*CACNA1A*
NG0362-III-1	35	?	M	Caucasian	Yes	BSP	*CACNA1A*
NG0369-II-2	80	58	F	Caucasian	Yes	BSP	*TOR2A, PCDH15, GTDC1*
NG0369-III-2	52	?	F	Caucasian	Yes	BSP	*TOR2A, PCDH15, GTDC1*
NG0369-III-6	46	?	F	Caucasian	Yes	BSP	*TOR2A, PCDH15, GTDC1*
NG0450-IV-3	80	53	F	Caucasian	Yes	BSP	*TRPV4, SERPINB9, CNTNAP2*
NG0450-V-4	64	40	F	Caucasian	Yes	BSP	*TRPV4, SERPINB9, CNTNAP2*
NG0450-V-6	51	38	M	Caucasian	Yes	writer's cramp	*TRPV4, SERPINB9, CNTNAP2*
NG1072-II-5	72	?	M	Caucasian	Yes	BSP	*ATP2A3*
NG1072-IV-2	24	21	F	Caucasian	Yes	cervical dystonia	*ATP2A3*

Abbreviations are as follows: AA, African-American

Table 2. Exome Coverage Otogenetics (Illumina)

Subjects	Exon Coverage ≥10x average	≥20x average	≥50x average	Mapped reads	Reads in exons (% of mapped)
NG0369-II-2	182,985 (98.71%)	180,451 (97.20%)	158,686 (85.48%)	40,359,835	27,882,382 (69.08%)
NG0369-III-2	183,285 (98.73%)	181,151 (97.58%)	164,561 (88.64%)	46,282,001	31,819,162 (68.75%)
NG0369-III-6	183,245 (98.71%)	181,036 (97.52%)	163,455 (88.05%)	45,818,817	31,595,919 (68.95%)
NG0450-V-4	183,339 (98.76%)	181,430 (97.73%)	167,149 (90.04%)	48,910,931	33,455,111 (68.41%)
NG0450-V-6	183,262 (98.72%)	180,540 (97.25%)	160,781 (86.61%)	44,674,009	30,667,372 (68.64%)
NG0450-IV-3	182,910 (98.53%)	180,235 (97.09%)	157,051 (84.60%)	38,518,463	26,893,126 (69.81%)
10012	183,177 (98.67%)	179,968 (96.94%)	151,762 (81.75%)	43,360,914	30,295,318 (69.86%)
10014	183,345 (98.76%)	180,745 (97.36%)	157,291 (84.73%)	45,133,245	30,866,426 (68.38%)
10035	183,449 (98.82%)	181,074 (97.54%)	159,805 (86.08%)	47,593,537	32,451,839 (68.18%)
10036	183,377 (98.78%)	180,492 (97.22%)	155,013 (83.50%)	43,455,430	29,831,744 (68.64%)
10043-II-2	182,658 (98.39%)	179,067 (96.46%)	149,939 (80.77%)	36,183,050	23,982,731 (66.28%)
10064	181,329 (97.67%)	174,416 (93.95%)	135,925 (73.22%)	31,906,497	23,887,178 (74.87%)
10076	181,156 (97.58%)	175,038 (94.29%)	137,975 (74.32%)	30,495,728	22,423,886 (73.53%)
10043-I-1	183,249 (98.71%)	181,131 (97.57%)	166,235 (89.54%)	50,010,351	34,444,302 (68.87%)
10178	183,260 (98.72%)	180,253 (97.10%)	157,001 (84.57%)	44,071,238	29,754,633 (67.51%)
10193	182,958 (98.55%)	179,944 (96.93%)	154,912 (83.44%)	40,787,072	27,819,791 (68.20%)
10274-II-3	183,257 (98.72%)	180,866 (97.43%)	162,983 (87.79%)	44,609,530	29,931,870 (67.09%)
10274-II-6	183,149 (98.66%)	181,247 (97.63%)	167,458 (90.2%)	54,207,882	36,192,334 (66.76%)
10455	183,030 (98.59%)	180,044 (96.98%)	156,811 (84.47%)	48,944,558	30,884,770 (63.10%)
10908-II-3	183,169 (98.67%)	181,017 (97.51%)	164,543 (88.63%)	47,084,143	32,159,148 (68.30%)
10908-III-9	183,065 (98.6%)	183,065 (97.35%)	163,351 (87.99%)	45,541,395	30,924,196 (67.90%)
25056	183,204 (98.68%)	180,273 (97.11%)	153,853 (82.87%)	45,212,675	30,858,562 (68.25%)
25069	182,022 (98.05%)	176,604 (95.13%)	142,875 (76.96%)	33,328,570	24,217,999 (72.66%)
25215	182,687 (98.41%)	179,180 (96.52%)	150,346 (80.99%)	37,771,677	25,469,621 (67.47%)
45263	183,442 (98.81%)	181,182 (97.61%)	163,127 (87.87%)	48,922,580	33,055,765 (67.56%)
85020	183,190 (98.68%)	180,786 (97.38%)	163,888 (88.28%)	58,478,165	35,599,118 (60.87%)

Table 3. Exome Coverage BGI (Complete Genomics)

Subject	Bases on targets	Targets covered ≥ 1X	Targets covered ≥ 5X	Targets covered ≥ 10X	Targets covered ≥ 20X
NG0362-III-1	58,970,115	99.56%	98.68%	97.64%	95.28%
NG1072-II-5	58,970,115	99.57%	98.72%	97.70%	95.36%
NG0362-II-2	58,970,115	99.56%	98.66%	97.60%	95.25%
NG0362-I-1	58,970,115	99.59%	98.76%	97.73%	95.32%
NG1072-IV-2	58,863,950	99.54%	98.66%	97.62%	95.27%

Table 4. Total and Filtered Variants

Pedigree (# subjects)	# common variants (SNVs + INDELs)	Potentially pathogenic variants							Platform
		Nonsynonymous SNVs	Nonsense SNVs	Synonymous SNVs	Splice site SNVs	Frame-shift	Other SNVs & indels	CNVs	
NG0362 (3)	30704	68	4	9	5	7	32	NA	Complete Genomics
NG1072 (2)	31417	63	1	8	4	5	42	NA	Complete Genomics
NG0369 (3)	3771	60	2	8	2	14	232	217	Illumina
NG0450 (3)	3749	48	3	8	0	13	214	145	Illumina
10043 (2)	4233	82	3	10	1	20	184	46	Illumina
10274 (2)	5462	141	6	10	2	25	26	110	Illumina
10908 (2)	4665	79	2	9	0	19	227	46	Illumina
10012 (1)	6511	118	3	9	1	6	243	60	Illumina
10014 (1)	7255	173	7	21	2	29	272	69	Illumina
10035 (1)	7016	141	7	16	4	23	251	38	Illumina
10036 (1)	6954	137	3	4	2	19	234	41	Illumina
10064 (1)	14196	258	5	36	9	30	347	50	Illumina
10076 (1)	14357	178	9	29	1	17	340	29	Illumina
10178 (1)	7865	127	8	21	2	33	239	14	Illumina
10193 (1)	7136	129	7	20	1	22	213	42	Illumina
10455 (1)	7551	167	7	24	1	25	262	80	Illumina
25056 (1)	7196	170	6	16	4	23	254	61	Illumina
25069 (1)	9064	145	4	22	3	23	254	11	Illumina
25215 (1)	7017	176	5	19	5	23	256	52	Illumina
45263 (1)	9340	139	2	19	3	25	277	25	Illumina
85020 (1)	7984	151	3	22	4	31	246	77	Illumina

Abbreviations are as follows: SNVs, single nucleotide variants; INDELs, small deletion and insertions; CNVs, copy number variants; NA, not available. SNVs and INDELs with (MAFs) > 0.001 (1 KG or EVS for Complete Genomics/BGI; and ExAC for Illumina/Otogenetics). Nonsynonymous SNVs: CADD phred score >15 or MetaLR > 0.75 or REVEAL > 0.5. Nonsense SNVs: CADD phred score > 15. Synonymous SNVs: CADD phred score > 15. Splice-site SNVs: CADD phred score > 15 or ada_score > 0.6 or rf_score > 0.6. Frame shift: CADD phred score > 15. Other SNVs & INDELs: CADD phred score > 15. CNVs: all generated via analysis with CNVkit.

Table 5. BSP-Associated Sequence Variants Identified with WES, *In Silico* Analyses, and Co-segregation Analyses

Pedigree	Phenotype	Gene	cDNA/Accession Number	Protein	ExAC	gnomAD	dbSNP	MutationTaster2	CADD	MetaLR	REVEL
10908	BSP+/BSP	*REEP4*	c.109C>T (NM_025232.3)	p.Arg37Trp	1.66E-05 (2/120748)	2.03E-05 (5/246118)	rs780399718	disease causing	34.0	0.960	0.767
NG0362	BSP	*CACNA1A*	c.7261_7262delinsGT (NM_001127222.1)	p.Pro2421Val	NA	NA	NA	disease causing	19.5	NA	NA
NG0369	BSP	*TOR2A*	c.568C>T (NM_130459.3)	p.Arg190Cys	5.84E-05 (7/119868)	4.07E-05 (10/245852)	rs376074923	disease causing	34.0	0.811	0.548
NG1072	BSP	*ATP2A3*	c.1966C>T (NM_005173.3)	p.Arg656Cys	5.51E-04 (66/119706)	6.63E-04 (183/276114)	rs140404080	disease causing	34.0	0.992	0.872
10043	BSP+	*GNA14*	c.989_990delCA (NM_004297.3)	p.Thr330Argfs Ter67	1.65E-05 (2/121284)	1.23E-05 (3/244472)	NA	disease causing	36.0	NA	NA
10043	BSP+	*HS1BP3*	c.94G>T (NM_022460.3)	p.Gly32Cys	NA	NA	NA	disease causing	34.0	0.803	0.454

Abbreviations are as follows: NA, not available.

Table 6. Candidate Genes Common to Two or More Pedigrees

Gene	Pedigree	Variant (Accession Number)	ExAC	gnomAD	dbSNP	MutationTaster2	CADD	MetaLR	REVEL
TRPV4	10274	c.1337G>T p.Arg446Leu (NM_021625.4)	2.64E-04 (32/121218)	2.93E-04 (81/276794)	rs143502097	disease causing	34.0	0.943	0.845
TRPV4	NG0450	c.745T>A p.Tyr249Asn (NM_001177431.1)	1.33E-04 (16/120694)	1.01E-04 (28/276982)	rs200210023	disease causing	27.7	0.876	0.779
TRPV4	10035	c.769C>G p.Leu257Val (NM_021625.4)	8.04E-04 (97/120672)	7.47E-04 (207/276982)	rs56217500	disease causing	23.8	0.958	0.669
CAPN11	10076	c.425T>C p.Leu142Pro (NM_007058.3)	NA	3.23E-05 (1/30926)	rs111320370	disease causing	32	0.982	0.918
CAPN11	10455	c.425T>C p.Leu142Pro (NM_007058.3)	NA	3.23E-05 (1/30926)	rs111320370	disease causing	32	0.982	0.918
DNAH17	10076	c.13295G>A p.Arg4432His (NM_173628.3)	6.60E-05 (8/121400)	6.89E-05 (19/275784)	rs775238626	disease causing	35	0.763	0.477
DNAH17	45263	c.9473C>T p.Pro3158Leu (NM_173628.3)	9.93E-05 (12/120872)	9.38E-05 (26/277132)	rs371315860	disease causing	25.3	0.947	0.613
VPS13C	10014	c.10954C>T p.Arg3652Ter (NM_020821.2)	1.84E-04 (21/120740)	1.85E-04 (50/270798)	rs138846118	disease causing	49	NA	NA
VPS13C	10455	c.9605C>G p.Ala3202Gly (NM_020821.2)	8.45E-06(1/118378)	4.55E-06 (1/219796)	rs750390167	disease causing	33	0.869	0.598
UNC13B	25069	c.4192A>G p.Thr1398Ala (NM_006377.3)	NA	NA	NA	disease causing	24	0.840	0.847
UNC13B	25215	c.4754G>A p.Arg1585His (NM_006377.3)	2.41E-04 (29/120560)	2.56E-04 (71/277062)	rs148652179	disease causing	34	0.952	0.644
SPTBN4	10012	c.1594G>A p.Glu532Lys (NM_020971.2)	4.16E-05 (5/120268)	6.16E-05 (17/275852)	rs201278278	disease causing	31	0.547	0.185
SPTBN4	10455	c.1543C>T p.Arg515Cys (NM_020971.2)	1.66E-05 (2/120186)	4.48E-05 (11/245642)	rs749869944	disease causing	34	0.584	0.316
MYOD1	10178	c.485C>T p.Ala162Val (NM_002478.4)	2.97E-04 (34/114390)	3.65E-04 (95/260404)	rs150053079	disease causing	23.1	0.977	0.678
MYOD1	10193	c.485C>T p.Ala162Val (NM_002478.4)	2.97E-04 (34/114390)	3.65E-04 (95/260404)	rs150053079	disease causing	23.1	0.977	0.678
MRPL15	10036	c.485_498delTAGCTATTGCTGCC p.Leu162HisfsTer109 (NM_014175.3)	NA	NA	NA	disease causing	35	NA	NA
MRPL15	10178	c.201delT p.Fhe67LeufsTer30 (NM_014175.3)	3.05E-04 (37/121336)	3.93E-04 (109/277238)	NA	disease causing	26.8	NA	NA

Abbreviations are as follows: ExAC, Exome Aggregation Consortium; CADD, Combined Annotation Dependent Depletion; REVEL, Rare Exome Variant Ensemble Learner; NA, not available.

Table 7. Confirmation of CNV variants using Digital PCR of Genomic DNA

Patient ID	Gene	hg19 CNV Coordinates	Log2Ratio	Digital PCR	
				Gene/RNASE P	CNV
10455	*BTNL3*	Chr5: 180416000-180429824	-0.95	0.50	Deletion
10036	*LILRA3*	Chr19: 54801997-54804319	-1.13	0.62	Deletion
10178	*LILRA3*	Chr19: 54801997- 54804319	-0.91	0.55	Deletion
10193	*LILRA3*	Chr19: 54801997- 54804319	-1.04	0.60	Deletion
25056	*SLC2A14*	Chr12: 7984292-8043706	0.53	1.52	Duplication
25056	*SLC2A3*	Chr12: 8074017- 8088678	0.53	1.51	Duplication
25215	*TOP3B*	Chr22: 22312829- 22330136	0.57	1.41	Duplication
85020	*UNK*	Chr17: 73808156- 73820465	0.58	1.50	Duplication
25056	*CLEC18B*	Chr16: 74443499- 74452124	-1.20	1.04	Normal
10036	*CYP2A7*	Chr19: 41381608- 41386459	-1.08	1.00	Normal
10036	*LRRC49*	Chr15: 71229066- 71305260	-0.92	1.05	Normal
10036	*RRP7A*	Chr22: 42908850- 42912408	-0.97	1.01	Normal
25056	*GOLGA8A*	Chr15: 34673679- 34681975	-0.93	1.45	Duplication
45263	*GOLGA8A*	Chr15: 34677244- 34681975	-0.94	1.08	Normal
85020	*GOLGA8A*	Chr15: 34677244- 34681975	-1.08	1.15	Normal

Table 8. Candidate Gene Literature Mining

Gene	Protein	Function	ExAC pLI	ExAC Missense Z-score	Diseases	Neural Localization*
CACNA1A	calcium channel, voltage-dependent, P/Q type, alpha 1A subunit	calcium ion transmembrane transport	1.00	7.23	SCA6, EA-2, hemiplegic migraine, dystonia	High expression in cerebellum, especially in Purkinje cells
REEP4	receptor accessory protein 4	microtubule-binding, endoplasmic reticulum and nuclear envelope protein	0.18	0.20	NA	Purkinje cells, cerebellar nuclear neurons
TOR2A	torsin family 2, member A	ATP binding	0.06	0.04	NA	Moderate expression in brain
ATP2A3	ATPase, Ca++ transporting, ubiquitous	calcium ion transport	0.06	3.13	NA	High expression in cerebellum, especially in Purkinje cells
GNA14	guanine nucleotide binding protein (G protein), alpha 14	adenylate cyclase-modulating G-protein coupled receptor signaling pathway	0.00	-0.25	NA	Moderate expression in brain
HS1BP3	HCLS1 binding protein 3	regulation of apoptotic process	0.00	-0.24	Associated with familial essential tremor	Moderate expression in brain
NEFH	neurofilament protein, heavy polypeptide	axon development	0.00	0.88	Charcot-Marie-Tooth disease Type 2CC, sporadic amyotrophic lateral sclerosis	High expression in cerebellum, especially in Purkinje cells
RWDD2A	RWD domain containing 2A	NA	0.00	0.64	NA	Moderate expression in brain
TRPV4	transient receptor potential cation channel, subfamily V, member 4	actin cytoskeleton reorganization, calcium ion transmembrane transport	0.00	3.12	Hereditary motor and sensory neuropathy, type IIc, brachyolmia type 3, metatropic dysplasia	Low expression in brain
SERPINB9	serpin family B member 9	cellular response to estrogen stimulus	0.00	-0.70	NA	Moderate expression in brain
CNTNAP2	contactin associated protein-like 2	neuron projection development	0.00	-0.91	Cortical dysplasia-focal epilepsy syndrome, Pitt-Hopkins like syndrome 1	High expression in brain
CAPN11	calpain 11	calcium-dependent cysteine-type endopeptidase activity	0.00	-0.82	NA	Low expression in brain
DNAH17	dynein, axonemal, heavy chain 17	cilium-dependent cell motility	NA	NA	NA	Low expression in brain
VPS13C	vacuolar protein sorting 13 homolog C	negative regulation of parkin-mediated stimulation of mitophagy in response to mitochondrial depolarization	0.00	-4.65	Parkinson disease	Moderate expression in brain
UNC13B	unc-13 homolog B	neurotransmitter secretion	0.00	0.51	NA	Moderate expression in brain
SPTBN4	spectrin, beta, non-erythrocytic 4	axon guidance	NA	NA	Myopathy, congenital, with neuropathy and deafness	High expression in brain
MYOD1	myogenic differentiation 1	skeletal muscle fiber development	0.00	1.96	NA	High expression in cerebellum
MRPL15	mitochondrial ribosomal protein L15	mitochondrial translational elongation	0.00	0.52	NA	Moderate expression in brain
BTNL3	butyrophilin-like protein 3	NA	0.04	1.31	NA	Low expression in brain
TOP3B	DNA topoisomerase 3-beta-1	Releases the supercoiling and torsional tension of DNA introduced during the DNA replication and transcription by transiently cleaving and rejoining one strand of the DNA duplex	0.11	3.18	NA	Moderate expression in brain
UNK	RING finger protein unkempt homolog	Sequence-specific RNA-binding protein which plays an important role in the establishment and maintenance of the early morphology of cortical neurons during embryonic development	0.99	3.85	NA	Moderate expression in brain

Abbreviations are as follows: ExAC, Exome Aggregation Consortium; CADD, Combined Annotation Dependent Depletion (v1.3); REVEL, Rare Exome Variant Ensemble Learner; NA, not available. *Based on Allen Brain Atlas, BioGPS and The Human Protein Atlas

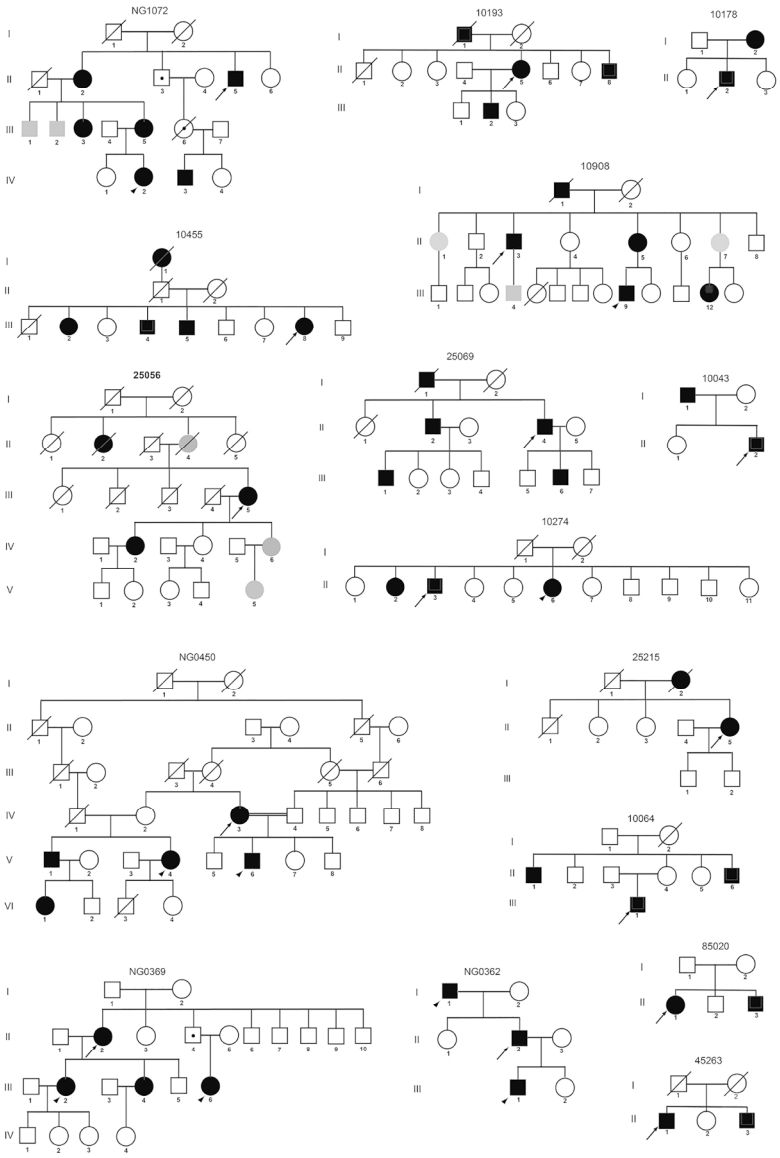

Figure 1

177x243mm (300 x 300 DPI)

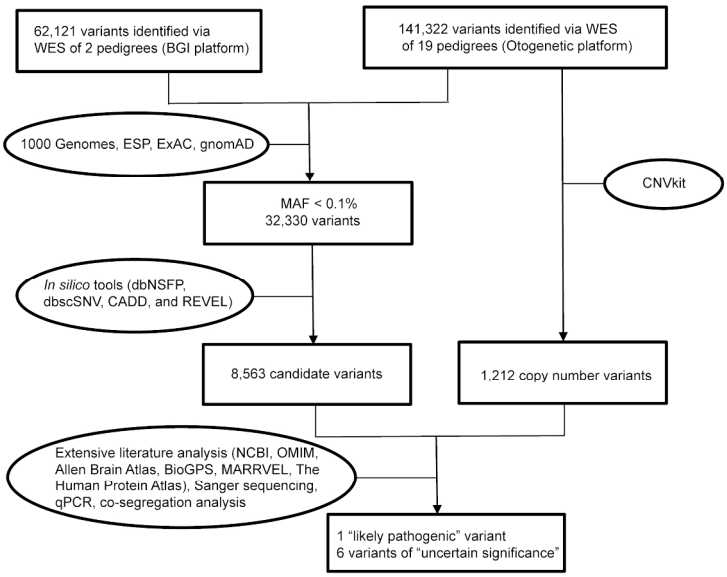

Figure 2

228x138mm (300 x 300 DPI)

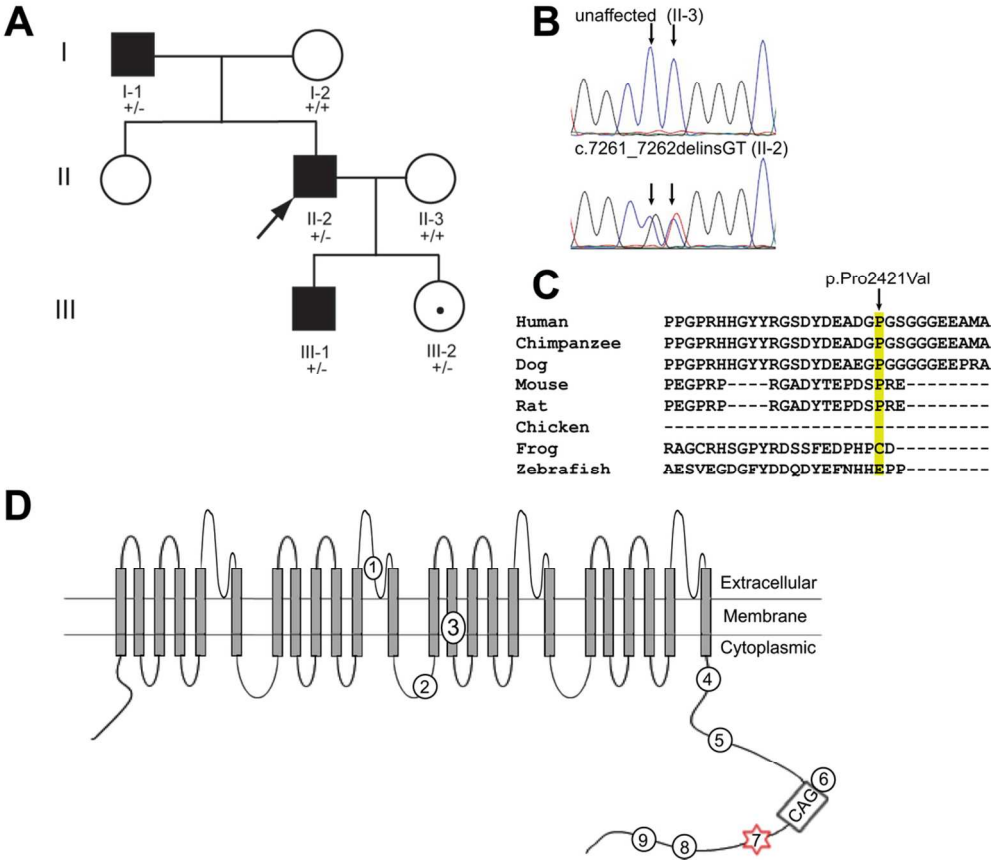

105x91mm (300 x 300 DPI)

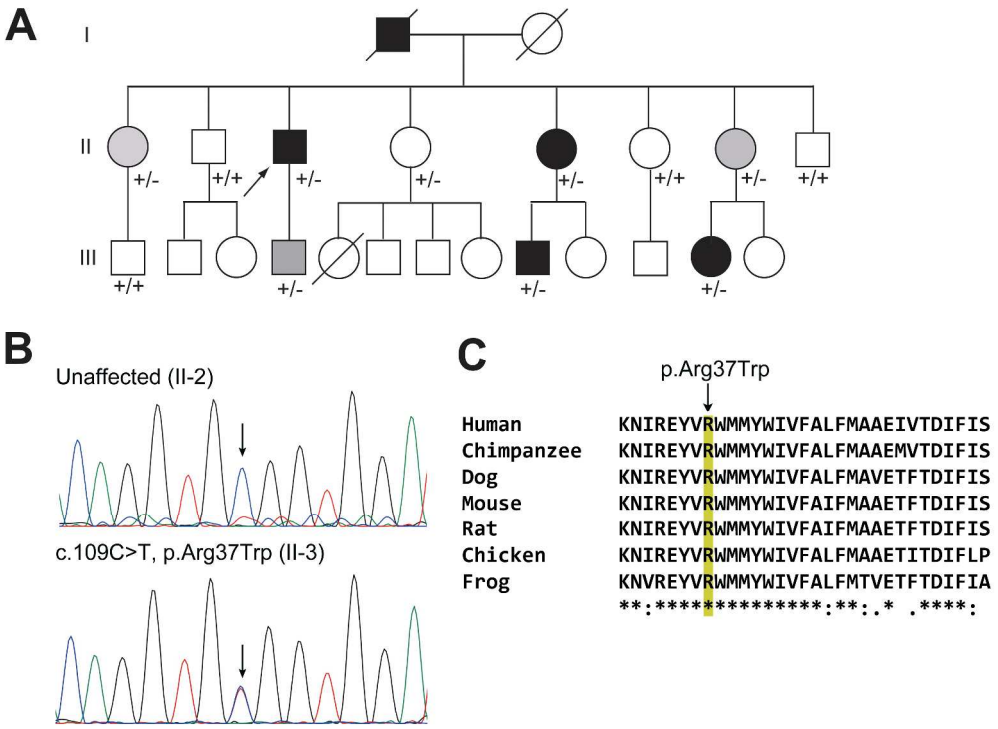

484x355mm (300 x 300 DPI)

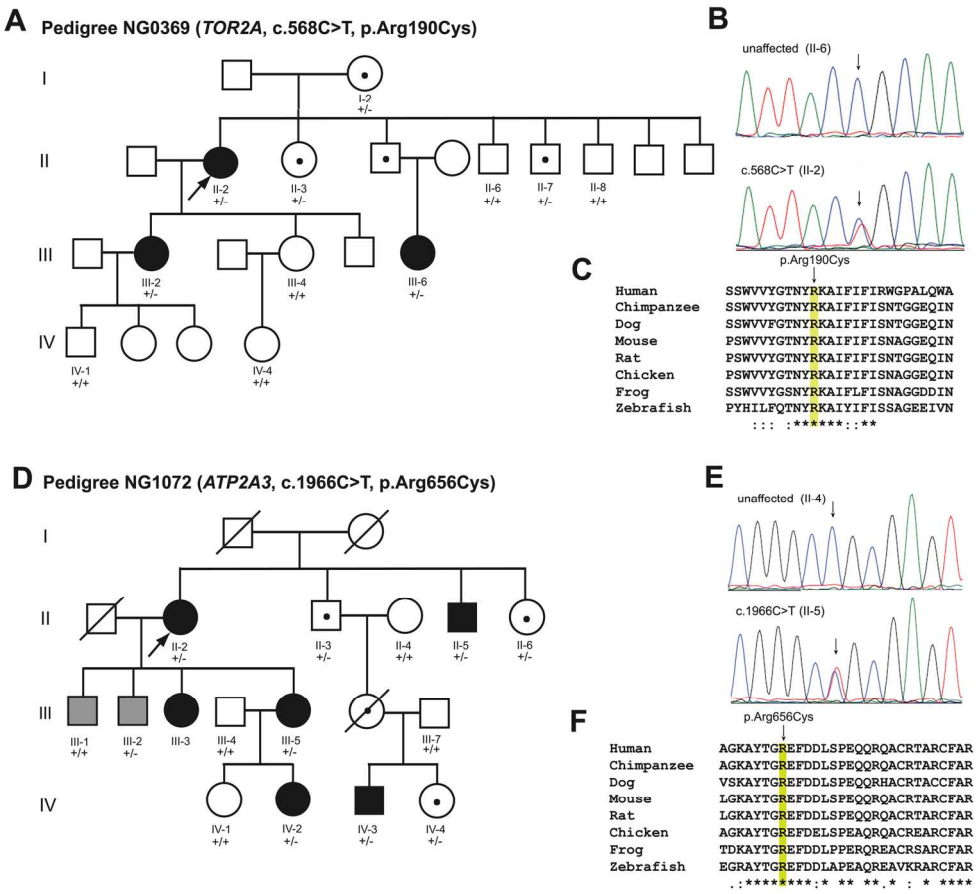

Figure 5

158x141mm (300 x 300 DPI)

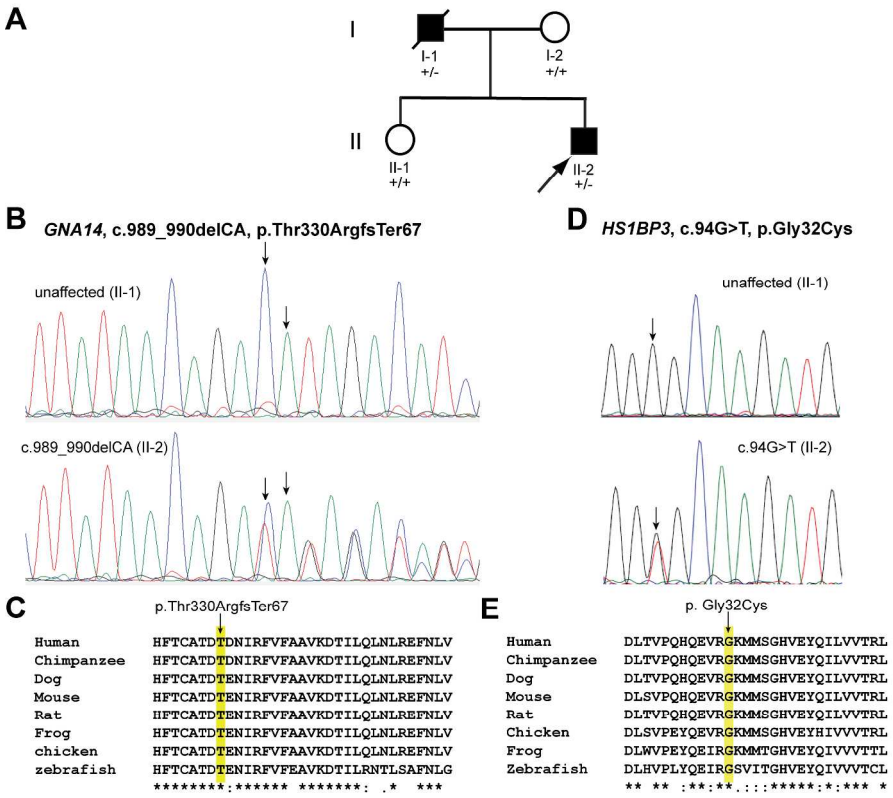

Figure 6

280x240mm (300 x 300 DPI)

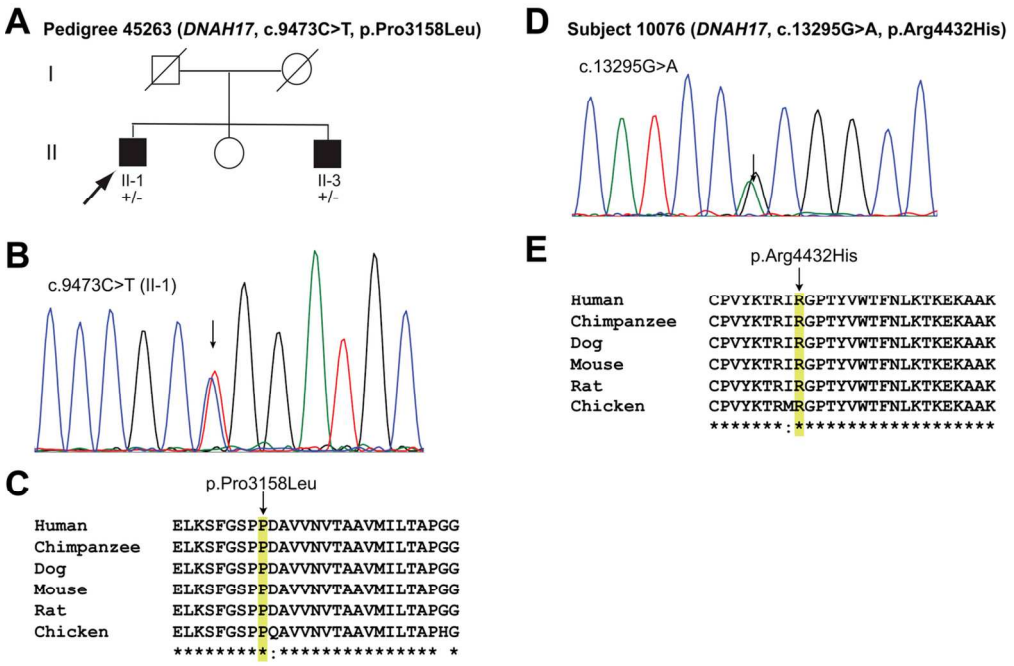

Figure 7

121x82mm (300 x 300 DPI)